General Disclaimer

One or more of the Following Statements may affect this Document

- This document has been reproduced from the best copy furnished by the organizational source. It is being released in the interest of making available as much information as possible.

- This document may contain data, which exceeds the sheet parameters. It was furnished in this condition by the organizational source and is the best copy available.

- This document may contain tone-on-tone or color graphs, charts and/or pictures, which have been reproduced in black and white.

- This document is paginated as submitted by the original source.

- Portions of this document are not fully legible due to the historical nature of some of the material. However, it is the best reproduction available from the original submission.

NASA

Technical Memorandum 86210

EARTH ALBEDO AND THE ORBIT OF LAGEOS

David Parry Rubincam and
Nelson R. Weiss

JUNE 1985

EARTH ALBEDO AND THE ORBIT
OF LAGEOS

by

David Parry Rubincam

Goddard Space Flight Center
Geodynamics Branch, Code 621
Greenbelt, Maryland 20771

and

Nelson R. Weiss

RMS Technologies
8201 Corporate Drive, Suite 500
Landover, Maryland 20785

EARTH ALBEDO AND THE ORBIT OF LAGEOS

David Parry Rubincam
Goddard Space Flight Center
Geodynamics Branch, Code 621
Greenbelt, Maryland 20771

and

Nelson R. Weiss
RMS Technologies
8201 Corporate Drive, Suite 500
Landover, Maryland 20785

Abstract. The long-period perturbations in the orbit of the Lageos satellite due to the earth's albedo have been found using a new analytical formalism. The earth is assumed to be a sphere whose surface diffusely reflects sunlight according to Lambert's law. Specular reflection is not considered. The formalism is based on spherical harmonics; it produces equations which hold regardless of whether the terminator is seen by the satellite or not. Specializing to the case of a realistic zonal albedo shows that Lageos' orbital semimajor axis changes periodically by only a few millimeters and the eccentricity by one part in 10^5. The longitude of the node increases secularly by about 3×10^{-4} arc sec yr^{-1}. The effect considered here can explain neither the secular decay of 1.1 mm day^{-1} in the semimajor axis nor the observed along-track variations in acceleration of order 2×10^{-12} ms^{-2}.

1. Introduction

This paper is concerned with an analytical treatment of what is commonly called "the albedo prob-lem", and how it relates to the orbit of the Lageos satellite.

The basic idea behind the albedo problem is this: sunlight is diffusely reflected by the earth up to an orbiting satellite. The radiation pressure of the incident light exerts a force on the satellite. The task is to find this force and its effect on the satellite's orbit. For an early review of the albedo problem, see Smith (1970). For some specific previous papers see Lochry (1966), and those cited in the next few paragraphs, as well as the ones cited by Smith (1970).

The albedo problem is important because reflected sunlight significantly perturbs the orbits of satellites with high surface-to-mass ratios, such as the balloon satellite Pageos (Prior, 1970; Laut-man, 1977a, 1977b; and Zerbini (1980).

It is also important to know how reflected sunlight affects the Lageos satellite, even though it is small and dense. A high-precision orbit is necessary for Lageos' mission of accurately measuring tectonic plate motion, polar motion, and length-of-day (Smith and Dunn, 1980). Smith (1983) has even speculated that the unexplained variations in along-track acceleration which have magnitude $\sim 2 \times 10^{-12}$ ms^{-2} (e.g., Rubincam and Weiss, 1985) are due to reflected sunlight. Anselmo et al. (1983) support this view, while Walch (1982) finds this mechanism to be about an order-of-magni-tude too small. Given this state of affairs, it is worthwhile to look further at the albedo problem and Lageos.

Solving the albedo problem analytically is not easy. Even though irradiance falls off with the inverse square of the distance, like gravity, the albedo problem has a number of complications not found in the gravitational problem: (a) The irradiance on the satellite depends on the orientation of the surface element doing the reflecting as well as the distance; an example is Lambert's law (e.g., Brown, 1965, p. 225); (b) The irradiance also depends on the solar zenith angle; (c) Only sur-face elements illuminated by the sun and visible from the satellite contribute to the force; (d) The earth's albedo varies with time, as well as latitude and longitude; (e) The atmosphere reflects and scatters light, so that one is not dealing with just reflection off the earth's surface; (f) The force depends on the properties and orientation of the satellite; generally a flat mirror will feel a dif-ferent force from a mottled ellipsoid, for example.

Given these complications, it is not surprising that Zerbini (1980) and Walch (1982) forsake the analytical approach of the other papers mentioned above for a numerical one. However, there are two good reasons for pursuing an analytical treatment: (i) equations give more insight into the problem than numerical methods, and (ii) equations can often lead to significant savings in com-puter time compared to numerical methods when integrating satellite orbits over time. Thus the rationale for the present work.

The complications (a) − (f) mentioned above are dealt with here as follows. The earth is assumed to be a sphere whose surface diffusely reflects light according to Lambert's law. The albedo variation on this surface is assumed to have a general spherical harmonic expansion whose coefficients may be functions of time. Spherical harmonics are also used to deal with solar illumination and the spherical cap seen by the satellite. The satellite itself is assumed to be a sphere of uniform albedo.

These assumptions lead to a vector equation for the albedo acceleration of the satellite. Then expressions for the orthogonal accelerations R, S, and W are found after specializing to the case of a zonal albedo variation (i.e., the earth albedo depends only on latitude). These accelerations are to be used in the Gaussian form of Lagrange's planetary equations; the acceleration equations have the virtue that they hold regardless of whether the satellite sees the terminator or not. Specializing still further to the case of Lageos and a realistic zonal albedo model based on Stephens et al. (1981) yields the following long-period results. The semimajor axis changes periodically with an amplitude of ~5 mm. The eccentricity changes periodically by about one part in 10^5. The longitude of the node increases secularly at the rate of about 3 x 10^{-4} arc sec yr^{-1}; periodic changes have amplitude ~ 3 x 10^{-4} arc sec, as do the changes in inclination. All of these effects are quite small. Lambertian reflection cannot account for the secular decrease of 1.1mm day^{-1} in the semimajor axis or the observed variations in along-track acceleration which have amplitude ~2 x 10^{-12} ms^{-2}.

Some notation is given in Tables I and II; other quantitities are defined in the text. A photograph of Lageos is shown in Figure 1.

2. Derivation of equations

In the case of the gravitational field, the usual method of obtaining the change in the Keplerian elements of the orbit with time is to first find the disturbing function and then use it in Lagrange's planetary equations (e.g., Kaula, 1966, pp. 25 - 37; Caputo, 1967, pp. 140 - 158). Unfortunately this approach cannot be used in the present problem where the reflected sunlight follows Lambert's law. The reason: the force cannot be written as the gradient of a potential, as it can for the case of the gravitational field. This is proved in Appendix 1. Hence no disturbing function exists. Instead the force must be dealt with directly. Once the force is found, it can be used in the Gaussian form of Lagrange's planetary equations, as is outlined below.

The derivation of the magnitude and direction of the force on a satellite due to diffusely reflected sunlight will now be given. Consider the inertial reference frame as shown in Figure 2. The origin is at the center of the earth. The frame does not rotate around with the earth. Suppose the sun shines on a surface element dS as shown in the figure. The sun is at position $\vec{r}_S$ while dS is

at $\vec{r}_A$. The surface element diffusely reflects some of the sunlight up to a satellite along $\vec{r}_L - \vec{r}_A$, where $\vec{r}_L$ is the satellite position. This light exerts an infinitesimal force $\vec{dF}$ on the satellite due to all of the sunlit surface elements visible to the satellite. This net force will be called the albedo force for short. Likewise the albedo force divided by the satellite mass will be called the albedo acceleration.

The albedo force depends on the shape, reflectivity and orientation of the satellite as well as on the characteristics of sunlight and the albedo of the earth. However, if the satellite is a perfect sphere with uniform reflectivity, the force $\vec{dF}$ will always act along the surface element-satellite line, in the direction away from $\vec{dS}$; in other words, along $\vec{r}_L - \vec{r}_A$ as shown in Figure 2. Such a case obviously greatly simplifies the treatment of the albedo force. Fortunately, Lageos satisfies these conditions to a very high degree of approximation (see Figure 1). Hence in the following the infinitesimal force $\vec{dF}$ will always be assumed in the dirction of $\vec{r}_L - \vec{r}_A$.

Now that the direction of $\vec{dF}$ has been established, its magnitude will be computed. Since the sunlight is assumed to be diffusely reflected according to Lambert's law, the radiance of dS, measured in watts per steradian per meter squared, is $N_R \cos \beta$ (e.g., Brown, 1965, pp. 220-225), where β is the colatitude in the local reference frame (x_1, y_1, z_1) of dS (see Figure 3) and N_R is a constant to be found next.

The radiant flux incident on dS is $F_S \cos \psi_S \, dS$, where F_S is the "solar constant" and ψ_S is the colatitude of the sun in the local frame of Figure 3. The amount of flux reflected by dS is $A(\theta, \lambda) F_S \cos \psi_S \, dS$, where $A(\theta, \lambda)$ is the albedo of dS, and (θ, λ) are the colatitude and longitude, respectively, in the inertial frame of Figure 2. This flux must be equal to $N_R \cos \beta \, dS$, integrated over the hemisphere into which dS diffusely reflects sunlight, assuming the power into the surface element equals the power out. Therefore

$$dS \int_0^{2\pi} \int_0^{\pi/2} N_R \cos \beta \, \sin\beta \, d\beta \, da = A(\theta, \lambda) F_S \cos \psi_S \, dS,$$

where a is the longitude in the local frame of Figure 3, so that

$$N_R = A(\theta, \lambda) F_S \cos \psi_S / \pi$$

The power $\dot{E}$ incident on the satellite due to dS is

$$\dot{E} = N_R \cos \psi_L \, dS \, d\Delta = A(\theta, \lambda) F_S \cos \psi_S \cos \psi_L \, dS \, d\Delta / \pi,$$

where ψ_L is the angle between $\vec{r}_L - \vec{r}_A$ and $\vec{r}_A$ (see Figure 2) and $d\Delta$ is the solid angle subtended by the satellite from dS. The magnitude of $\vec{dF}$ can be found from $\dot{E}$ in the following manner. The inci-

3

dent momentum p of the light is related to its energy E by E = pc, where c is the speed of light (e.g., Alonso and Finn, 1968, p. 14). The incident momentum per unit time is thus $\dot{E}/c$. The force on the satellite is the change in its momentum per unit time, and is given by $C_R \dot{E}/c$ (e.g., Rubincam and Weiss, 1985), where C_R is the radiation coefficient. (If the satellite absorbs all of the incident light and re-radiates it isotropically, then $C_R = 1$. If the satellite is a flat, perfect mirror reflecting the incident light straight back, then $C_R = 2$. So $1 \leqslant C_R \leqslant 2$. For Lageos, $C_R = 1.13$). The magnitude of $\overrightarrow{dF}$ is therefore

$$|\overrightarrow{dF}| = \frac{C_R F_S}{\pi c} A(\theta,\lambda) \cos \psi_S \cos \psi_L \, dS \, d\Delta. \tag{1}$$

The vector force $\overrightarrow{dF}$ can be found by multiplying (1) by the unit vector $(\overrightarrow{r_L} - \overrightarrow{r_A})/|\overrightarrow{r_L} - \overrightarrow{r_A}|$. Also, for a spherical satellite of radius R_L, $d\Delta \approx \pi R_L^2 / |\overrightarrow{r_L} - \overrightarrow{r_A}|^2$ to an incredible degree of accuracy, since $R_L \ll |\overrightarrow{r_L} - \overrightarrow{r_A}|$ always. Further,

$$\cos \psi_S = (\overrightarrow{r_S} - \overrightarrow{r_A}) \cdot \overrightarrow{r_A} / (|\overrightarrow{r_S} - \overrightarrow{r_A}| \cdot |\overrightarrow{r_A}|) \approx \overrightarrow{r_S} \cdot \overrightarrow{r_A} / (|\overrightarrow{r_S}| \cdot |\overrightarrow{r_A}|)$$

because $|\overrightarrow{r_A}| \ll |\overrightarrow{r_S}|$, since the sun is so far away from the earth. Likewise, $F_S \approx F_S^o (a_S/|\overrightarrow{r_S}|)^2$, where a_S is the semimajor axis of the earth's orbit about the sun and F_S^o is a constant, equal to about 1376 W m^{-2} (Hickey et al., 1980). No such approximation can be used for $\cos \psi_L$, so it is $(\overrightarrow{r_L} - \overrightarrow{r_A}) \cdot \overrightarrow{r_A}/(|\overrightarrow{r_L} - \overrightarrow{r_A}| \cdot |\overrightarrow{r_A}|)$ exactly.

The albedo force $\overrightarrow{F}$ can be found by substituting the formulae above into (1) and integrating over area yielding

$$\overrightarrow{F} = M_L \ddot{\overrightarrow{r_L}} = \frac{C_R R_L^2 F_S^o}{c} \left(\frac{a_S^2}{|\overrightarrow{r_S}|^3}\right) \cdot \int_\Xi \frac{A(\theta,\lambda) [\overrightarrow{r_S} \cdot \overrightarrow{r_A}] [(\overrightarrow{r_L} - \overrightarrow{r_A}) \cdot \overrightarrow{r_A}] [\overrightarrow{r_L} - \overrightarrow{r_A}]}{|\overrightarrow{r_L} - \overrightarrow{r_A}|^4 \, |\overrightarrow{r_A}|^2} \, dS \tag{2}$$

in vector notation where $\ddot{\overrightarrow{r_L}}$ is the albedo acceleration in the reference frame of Figure 2, M_L is the satellite mass, and Ξ is the sunlit portion of the earth visible to the satellite. The albedo acceleration can be written

4

$$\ddot{\vec{r}}_L = \frac{C_R R_L^2 F_S^{\circ}}{cM_L} \left(\frac{a_S}{r_S}\right)^2 \rho^2 \cdot \iint_{\Xi} \frac{A(\theta,\lambda) \cos \psi_S (\cos \eta - \rho)}{(1 - 2\rho \cos \eta + \rho^2)^2}$$

$$\cdot [(\sin \theta_L \cos \lambda_L - \rho \sin\theta \cos\lambda)\hat{x}$$

$$+ (\sin \theta_L \sin \lambda_L - \rho \sin\theta \sin\lambda)\hat{y} \tag{3}$$

$$+ (\cos \theta_L - \rho \cos\theta)\hat{z}] \sin\theta \; d\theta \; d\lambda$$

after reverting back to trigonometric notation. Here η is the angle betwen $\vec{r}_L$ and $\vec{r}_A$ (see Figure 2), so that $\cos \eta = \cdot \vec{r}_L \cdot \vec{r}_A / (|\vec{r}_L| \cdot |\vec{r}_A|)$, $R_A = |\vec{r}_A|$, $r_L = |\vec{r}_L|$, $r_S = |\vec{r}_S|$, and $\rho = R_A/r_L$. Also, $dS = R_A^2 \sin\theta \; d\theta \; d\lambda$, and (θ_L, λ_L) are the colatitude and longitude of the satellite respectively in the frame of Figure 2, whereas $(\hat{x}, \hat{y}, \hat{z})$ are the unit vectors along the appropriate axes in the frame of Figure 2. A spherical earth of radius R_A is assumed in (3); R_A is the distance from the center of the earth to the "top of the atmosphere". The "top of the atmosphere" is taken to be 10 km above the surface (the height of the troposphere) so that R_A = 6371 km + 10 km = 6381 km, where 6371 km is the radius of a sphere with the same volume as the earth. (A more common choice for the top of the atmosphere is 30 km; e.g., Bess and Smith, 1981.)

The task ahead is to make the integral in (3) tractable. Spherical harmonics form a viable approach, as shown below.

Suppose a function D is defined so that

$$D = \begin{cases} \cos \psi_S & 0 \leqslant \psi_S \leqslant \frac{\pi}{2} \\ \\ 0 & \frac{\pi}{2} \leqslant \psi_S \leqslant \pi \end{cases}$$

then D can be written as an infinite sum of Legendre polynomials

$$D = \sum_{L=0}^{\infty} d_L P_L (\cos \psi_S)$$

where $P_L (\cos \psi_S)$ is the Legendre polynomial of degree L and the d_L are the appropriate coefficients. (The subscript should not be confused with that used for the satellite.) The addition theorem for spherical harmonics

5

$$P_L(\cos\psi_S) = \frac{4\pi}{2L+1} \sum_{J=-L}^{+L} Y_L^{J*}(\theta_S, \lambda_S)\, Y_L^J(\theta, \lambda)$$

(e.g., Merzbacher, 1970, p. 189) can be used in the above equation to write

$$D(\theta, \lambda, \theta_S, \lambda_S) = 4\pi \sum_{L=0}^{\infty} \sum_{J=-L}^{+L} \left(\frac{d_L}{2L+1}\right) Y_L^{J*}(\theta_S, \lambda_S)\, Y_L^J(\theta, \lambda) \qquad (4)$$

where the

$$Y_L^J(\theta, \lambda) = (-1)^{\frac{J+|J|}{2}} \left[\frac{(2L+1)(L-|J|)!}{4\pi(L+|J|)!}\right]^{\frac{1}{2}} P_{L,|J|}(\cos\theta)\, e^{iJ\lambda}$$

are the spherical harmonics used in quantum mechanics (Merzbacher, 1970, p. 185), and (θ_S, λ_S) are the respective colatitude and longitude of the sun in the frame of Figure 2. Here $P_{L,|J|}(\cos\theta)$ is the associated Legendre polynomial of degree L and order $|J|$ and $i = \sqrt{-1}$. The asterisk (*) denotes the complex conjugate and $-L \leqslant J \leqslant +L$. The quantum-mechanical spherical harmonics have normalization

$$\int_0^{2\pi}\int_0^\pi Y_L^{J*}(\theta, \lambda)\, Y_{L'}^{J'}(\theta, \lambda)\, \sin\theta\, d\theta\, d\lambda = \delta_{JJ'}\delta_{LL'}$$

(Merzbacher, 1970, p. 186) where $\delta_{JJ'}$ is the Kronecker delta. The relation between the quantum-mechanical spherical harmonics and those commonly used in geophysics is given in Appendix 2.

Likewise a function B defined so that

$$B = \begin{cases} \dfrac{\cos\eta - \rho}{[1 - 2\rho\cos\eta + \rho^2]^2} & 0 \leqslant \eta \leqslant \text{Arc}\cos(\rho) \\[2em] 0 & \text{Arc}\cos(\rho) < \eta \leqslant \pi \end{cases}$$

can also be written

$$B = \sum_{\ell=0}^{\infty} b_\ell P_\ell(\cos\eta)$$

6

so that

$$B(\theta,\lambda,\theta_L,\lambda_L) = 4\pi \sum_{\ell=0}^{\infty} \left(\frac{b_\ell}{2\ell+1}\right) Y_\ell^{m*}(\theta_L,\lambda_L) \, Y_\ell^m(\theta,\lambda) \tag{5}$$

where the b_ℓ depend on ρ. Arc $\cos(\rho)$ is the angular radius of the cap visible to the satellite. Finding the d_L and the b_ℓ will be postponed until after a general expression for the albedo acceleration is derived.

Now $D(\theta, \lambda, \theta_S, \lambda_S)$ is zero over the night hemisphere of the earth. Also, $B(\theta, \lambda, \theta_L, \lambda_L)$ is zero outside the spherical cap visible to the satellite. Hence by substituting $D(\theta, \lambda, \theta_S, \lambda_S)$ for $\cos \psi_S$ and $B(\theta, \lambda, \theta_L, \lambda_L)$ for $(\cos \eta - \rho)/[1 - 2\rho \cos \eta + \rho^2]^2$ in (3) allows ... area of integration to be changed from Ξ to the entire sphere, since now the integrand is zero outside the region Ξ. This enlargement in the area of integration greatly simplifies the evaluation of the integral, as will be seen shortly.

The albedo $A(\theta, \lambda)$ is also assumed to have a spherical harmonic expansion:

$$A(\theta,\lambda) = \sum_{N=0}^{\infty}{}' \sum_{K=-N}^{+N} \hat{A}_N^{K*} \, Y_N^{K*}(\theta,\lambda), \tag{6}$$

where the coefficients $\hat{A}_N^{K*}$ refer to the inertial reference frame of Figure 2. The albedo is defined over the entire earth, regardless of day or night. This should cause no conceptual difficulties; the values associated with the night side may be thought of as those the albedo would take if the sun could somehow be made to shine on the sunless hemisphere. Further, $0 \leqslant A(\theta, \lambda) \leqslant 1$.

Now realizing that

$$\cos \lambda = \frac{e^{+i\lambda} + e^{-i\lambda}}{2}$$

$$\sin \lambda = \frac{e^{+i\lambda} - e^{-i\lambda}}{2i}$$

and using the properties

7

$$\cos\theta\ Y_\ell^m(\theta,\lambda) = \sqrt{\frac{(\ell-m+1)(\ell+m+1)}{(2\ell+1)(2\ell+3)}}\ Y_{\ell+1}^m(\theta,\lambda) + \sqrt{\frac{(\ell-m)(\ell+m)}{(2\ell-1)(2\ell+1)}}\ Y_{\ell-1}^m(\theta,\lambda)$$

$$\sin\theta\ e^{+i\lambda}\ Y_\ell^m(\theta,\lambda) = -\sqrt{\frac{(\ell+m+1)(\ell+m+2)}{(2\ell+1)(2\ell+3)}}\ Y_{\ell+1}^{m+1}(\theta,\lambda)$$

$$+\sqrt{\frac{(\ell-m-1)(\ell-m)}{(2\ell-1)(2\ell+1)}}\ Y_{\ell-1}^{m+1}(\theta,\lambda)$$

$$\sin\theta\ e^{-i\lambda}\ Y_\ell^m(\theta,\lambda) = \sqrt{\frac{(\ell-m+1)(\ell-m+2)}{(2\ell+1)(2\ell+3)}}\ Y_{\ell+1}^{m-1}(\theta,\lambda)$$

$$-\sqrt{\frac{(\ell+m-1)(\ell+m)}{(2\ell-1)(2\ell+1)}}\ Y_{\ell-1}^{m-1}(\theta,\lambda)$$

(e.g. Merzbacher, 1970, p. 187) allows one to write from (5)

$$B(\theta,\lambda\theta_L,\lambda_L)(\sin\theta_L\cos\theta_L - \rho\sin\theta\cos\lambda) = 2\pi \sum_{\ell=0}^{\infty} \sum_{m=-\ell}^{+\ell}\ Y_\ell^{m*}(\theta_L,\lambda_L)$$

$$\left\{ -\left[\left(\frac{b_{\ell-1}}{2\ell-1}\right) - \rho\left(\frac{b_\ell}{2\ell+1}\right)\right] \sqrt{\frac{(\ell+m-1)(\ell+m)}{(2\ell-1)(2\ell+1)}}\ Y_{\ell-1}^{m-1}(\theta,\lambda) \right.$$

$$\left. +\left[\left(\frac{b_{\ell-1}}{2\ell-1}\right) - \rho\left(\frac{b_\ell}{2\ell+1}\right)\right] \sqrt{\frac{(\ell-m-1)(\ell-m)}{(2\ell-1)(2\ell+1)}}\ Y_{\ell-1}^{m+1}(\theta,\lambda) \right.$$

8

$$+ \left[\left(\frac{b_{\ell+1}}{2\ell+3}\right) - \rho\left(\frac{b_\ell}{2\ell+1}\right)\right] \sqrt{\frac{(\ell-m+1)(\ell-m+2)}{(2\ell+1)(2\ell+3)}} \; Y_{\ell+1}^{m-1}(\theta,\lambda)$$

$$\left. - \left[\left(\frac{b_{\ell+1}}{2\ell+3}\right) - \rho\left(\frac{b_\ell}{2\ell+1}\right)\right] \sqrt{\frac{(\ell+m+1)(\ell+m+2)}{(2\ell+1)(2\ell+3)}} \; Y_{\ell+1}^{m+1}(\theta,\lambda) \right\}$$

after gathering coefficients of $Y_\ell^{m*}(\theta_L, \lambda_L)$. (Interestingly, there is no danger of the superscripts or subscripts of the $Y_{\ell\pm1}^{m\pm1}(\theta,\lambda)$ exceeding their proper limits in the above equation; the radical in front of such terms is zero.)

Using the equation above, similar equations for $B(\theta,\lambda,\theta_L,\lambda_L)$ ($\sin\theta_L\sin\lambda_L - \rho\sin\theta\sin\lambda$) and $B(\theta,\lambda,\theta_L,\lambda_L)$ ($\cos\theta_L - \rho\cos\theta$), as well as (4) and (6) in (3) and integrating over the whole sphere yields

$$\ddot{\vec{r}}_L = \frac{4\pi^{3/2} C_R R_L^2 F_S^\circ}{c M_L} \left(\frac{a_S}{r_S}\right)^2 \rho^2$$

$$\cdot \sum_{N=0}^{\infty} \sum_{K=-N}^{+N} \sum_{L=0}^{\infty} \sum_{J=-L}^{+L} \sum_{\ell=0}^{\infty} \sum_{m=-\ell}^{+\ell} (-1)^K \left[\frac{2N+1}{(2\ell+1)(2L+1)}\right]^{1/2} d_L \hat{A}_N^{K*} Y_L^J(\theta_S,\lambda_S) Y_\ell^{m*}(\theta_L,\lambda_L)$$

$$\cdot \left[\left\{-\left[\left(\frac{b_{\ell-1}}{2\ell-1}\right) - \rho\left(\frac{b_\ell}{2\ell+1}\right)\right]\sqrt{(\ell+m-1)(\ell+m)} \begin{pmatrix} N & L & \ell-1 \\ -K & J & m-1 \end{pmatrix} \begin{pmatrix} N & L & \ell-1 \\ 0 & 0 & 0 \end{pmatrix}\right.\right.$$

$$+ \left[\left(\frac{b_{\ell-1}}{2\ell-1}\right) - \rho\left(\frac{b_\ell}{2\ell+1}\right)\right]\sqrt{(\ell-m-1)(\ell-m)} \begin{pmatrix} N & L & \ell-1 \\ -K & J & m+1 \end{pmatrix} \begin{pmatrix} N & L & \ell-1 \\ 0 & 0 & 0 \end{pmatrix}$$

$$+ \left[\left(\frac{b_{\ell+1}}{2\ell+3}\right) - \rho\left(\frac{b_\ell}{2\ell+1}\right)\right]\sqrt{(\ell-m+1)(\ell-m+2)} \begin{pmatrix} N & L & \ell+1 \\ -K & J & m-1 \end{pmatrix} \begin{pmatrix} N & L & \ell+1 \\ 0 & 0 & 0 \end{pmatrix}$$

9

$$-\left[\left(\frac{b_{\ell+1}}{2\ell+3}\right)-\rho\left(\frac{b_\ell}{2\ell+1}\right)\right]\sqrt{(\ell+m+1)(\ell+m+2)}\ \begin{pmatrix} N & L & \ell+1 \\ & & \\ -K & J & m+1 \end{pmatrix}\begin{pmatrix} N & L & \ell+1 \\ & & \\ 0 & 0 & 0 \end{pmatrix}\Bigg\}\hat{x}$$

$$+\frac{1}{i}\Bigg\{+\left[\left(\frac{b_{\ell-1}}{2\ell-1}\right)-\rho\left(\frac{b_\ell}{2\ell+1}\right)\right]\sqrt{(\ell+m-1)(\ell+m)}\ \begin{pmatrix} N & L & \ell-1 \\ & & \\ -K & J & m-1 \end{pmatrix}\begin{pmatrix} N & L & \ell-1 \\ & & \\ 0 & 0 & 0 \end{pmatrix}$$

$$+\left[\left(\frac{b_{\ell-1}}{2\ell-1}\right)-\rho\left(\frac{b_\ell}{2\ell+1}\right)\right]\sqrt{(\ell-m-1)(\ell-m)}\ \begin{pmatrix} N & L & \ell-1 \\ & & \\ -K & J & m+1 \end{pmatrix}\begin{pmatrix} N & L & \ell-1 \\ & & \\ 0 & 0 & 0 \end{pmatrix}$$

$$-\left[\left(\frac{b_{\ell+1}}{2\ell+3}\right)-\rho\left(\frac{b_\ell}{2\ell+1}\right)\right]\sqrt{(\ell-m+1)(\ell-m+2)}\ \begin{pmatrix} N & L & \ell+1 \\ & & \\ -K & J & m-1 \end{pmatrix}\begin{pmatrix} N & L & \ell+1 \\ & & \\ 0 & 0 & 0 \end{pmatrix}$$

$$-\left[\left(\frac{b_{\ell+1}}{2\ell+3}\right)-\rho\left(\frac{b_\ell}{2\ell+1}\right)\right]\sqrt{(\ell+m+1)(\ell+m+2)}\ \begin{pmatrix} N & L & \ell+1 \\ & & \\ -K & J & m+1 \end{pmatrix}\begin{pmatrix} N & L & \ell+1 \\ & & \\ 0 & 0 & 0 \end{pmatrix}\Bigg\}\hat{y}$$

$$+2\Bigg\{\left[\left(\frac{b_{\ell-1}}{2\ell-1}\right)-\rho\left(\frac{b_\ell}{2\ell+1}\right)\right]\sqrt{(\ell-m)(\ell+m)}\ \begin{pmatrix} N & L & \ell-1 \\ & & \\ -K & J & m \end{pmatrix}\begin{pmatrix} N & L & \ell-1 \\ & & \\ 0 & 0 & 0 \end{pmatrix}$$

$$+\left[\left(\frac{b_{\ell+1}}{2\ell+3}\right)-\rho\left(\frac{b_\ell}{2\ell+1}\right)\right]\sqrt{(\ell-m+1)(\ell+m+1)}\ \begin{pmatrix} N & L & \ell+1 \\ & & \\ -K & J & m \end{pmatrix}\begin{pmatrix} N & L & \ell+1 \\ & & \\ 0 & 0 & 0 \end{pmatrix}\Bigg\}\hat{z}\Bigg] \quad (7)$$

for the albedo acceleration, where

$$\int_0^{2\pi} \int_0^{\pi} Y_N^{*K}(\theta,\lambda) \, Y_L^{J}(\theta,\lambda) \, Y_\ell^{m}(\theta,\lambda) \, \sin\theta \; d\theta \; d\lambda$$

$$= (-1)^K \left[\frac{(2N+1)(2L+1)(2\ell+1)}{4\pi} \right]^{\frac{1}{2}} \begin{pmatrix} N & L & \ell \\ -K & J & m \end{pmatrix} \begin{pmatrix} N & L & \ell \\ 0 & 0 & 0 \end{pmatrix}$$

(e.g., Rotenberg, et al., 1959, p. 5) is the simplification of the integration mentioned earlier. The two-row arrays are the 3-j symbols of quantum mechanics (e.g., Rotenberg et al., 1959, p. 2)

$$\begin{pmatrix} j_1 & j_2 & j_3 \\ m_1 & m_2 & m_3 \end{pmatrix} = (-1)^{j_1 - j_2 - m_3}$$

$$\times \left(\frac{(j_1 + j_2 - j_3)! \, (j_1 - j_2 + j_3)! \, (-j_1 + j_2 + j_3)! \, (j_1 + m_1)! \, (j_1 - m_1)! \, (j_2 + m_2)! \, (j_2 - m_2)! \, (j_3 + m_3)! \, (j_3 - m_3)!}{(j_1 + j_2 + j_3 + 1)!} \right)^{\frac{1}{2}}$$

$$\sum_k \frac{(-1)^k}{k!(j_1 + j_2 - j_3 - k)! \, (j_1 - m_1 - k)! \, (j_2 + m_2 - k)! \, (j_3 - j_2 + m_1 + k)! \, (j_3 - j_1 - m_2 + k)!} \, .$$

The sum in this equation is over all values of k so as to make the right side meaningful. The 3-j symbol is automatically zero unless the triangle inequalities

$$j_1 + j_2 - j_3 \geqslant 0$$

$$j_1 - j_2 + j_3 \geqslant 0$$

$$-j_1 + j_2 + j_3 \geqslant 0$$

are satisfied (Rotenberg et al., 1959, p. 3). The 3-j symbols also have the following properties:

$$\begin{pmatrix} j_1 & j_2 & j_3 \\ m_1 & m_2 & m_3 \end{pmatrix} = 0 \qquad \text{for } m_1 + m_2 + m_3 \neq 0 \tag{8}$$

11

so that

$$(-1)^{m_1+m_2+m_3}\begin{pmatrix} j_1 & j_2 & j_3 \\ m_1 & m_2 & m_3-1 \end{pmatrix} = (-1)\begin{pmatrix} j_1 & j_2 & j_3 \\ m_1 & m_2 & m_3-1 \end{pmatrix} \tag{9}$$

for example, and

$$\begin{pmatrix} j_1 & j_2 & j_3 \\ -m_1 & -m_2 & -m_3 \end{pmatrix} = (-1)^{j_1+j_2+j_3}\begin{pmatrix} j_1 & j_2 & j_3 \\ m_1 & m_2 & m_3 \end{pmatrix} \tag{10}$$

(Rotenberg et al., 1959, pp. 2-3). These properties will be used shortly.

The albedo acceleration $\vec{r}_L$ of the satellite will next be expressed in terms of the orbit parameters.

First assume that the albedo variations are attached to the earth, i.e., the light and dark markings rotate around with it. In this case the coefficients of (6) can be written

$$\hat{A}_N^K = A_N^K \; e^{-iK\Theta} \tag{11}$$

where the A_N^K are now the earth-fixed coefficients and Θ is Greenwich sidereal time. The right-handed earth-fixed frame has its x-axis intersecting the equator at the Greenwich meridian and its z-axis piercing the north pole.

It can easily be shown from the standard development of the gravitational potential (e.g., Caputo, 1967, pp. 140-145; beware of typographical errors) that

$$Y_\ell^m(\theta,\lambda) = \frac{(-1)^{\frac{m+|m|}{2}}}{2[\pi(2-\delta_{om})]^{1/2}}$$

$$\cdot \sum_{p=0}^{\ell} F_{\ell|m|p}(I) \begin{cases} e^{i(2\delta_{m|m|}-1)[(\ell-2p)(\omega+f)+|m|\Omega]} & \ell-m \text{ even} \\ \\ \dfrac{(2\delta_{m|m|}-1)}{i} e^{i(2\delta_{m|m|}-1)[(\ell-2p)(\omega+f)+|m|\Omega]} & \\ & \ell-m \text{ odd} \end{cases} \tag{12}$$

12

In this equation $\overline{F}_{\ell mp}(I)$ is the normalized inclination function

$$\overline{F}_{\ell mp}(I) = \left[\frac{(2-\delta_{om})(2\ell+1)(\ell-m)!}{(\ell+m)!} \right] F_{\ell mp}(I)$$

(Rubincam, 1982, p. 364), while I is the inclination of the satellite orbit with respect to the earth's equator, Ω the position of the orbit node on the equator, ω the argument of perigee, and f the true anomaly.

Using (11), (12), and the succeeding equation, one can write

$$A_N^{K*} \, Y_L^{J*}(\theta_S, \lambda_S) \, Y_\ell^{m*}(\theta, \lambda)$$

$$= \frac{(-1)^{\frac{K+|K|+J+|J|+m+|m|}{2}}}{4\pi^{1/2}} \left[\frac{(2-\delta_{oK})}{(2-\delta_{oJ})(2-\delta_{om})} \right]^{1/2} \sum_{h=0}^{L} \sum_{p=0}^{\ell} \overline{F}_{L|J|h}(I_S) \overline{F}_{\ell|m|p}(I)$$

$$\cdot \, e^{+i \left\{ (1-2\delta_{J|J|}) [(L-2h)(\omega_S+f_S) + |J|\Omega_S] + (1-2\delta_{m|m|})[(\ell-2p)(\omega+f) + |m|\Omega] + K\Theta \right\}}$$

$$\cdot \left\{ \begin{array}{ll}
\overline{A}_{N|K|1} - i(1-2\delta_{K|K|})\overline{A}_{N|K|2} & \text{I:} \quad \begin{array}{l} L-J \text{ even} \\ \ell-m \text{ even} \end{array} \\[2ex]
\dfrac{(1-2\delta_{m|m|})}{i}\overline{A}_{N|K|1} - (1-2\delta_{K|K|})(1-2\delta_{m|m|})\overline{A}_{N|K|2} & \text{II:} \quad \begin{array}{l} L-J \text{ even} \\ \ell-m \text{ odd} \end{array} \\[2ex]
\dfrac{(1-2\delta_{J|J|})}{i}\overline{A}_{N|K|1} - (1-2\delta_{K|K|})(1-2\delta_{J|J|})\overline{A}_{N|K|2} & \text{III:} \quad \begin{array}{l} L-J \text{ odd} \\ \ell-m \text{ even} \end{array} \\[2ex]
-(1-2\delta_{J|J|})(1-2\delta_{m|m|})\overline{A}_{N|K|1} + i(1-2\delta_{K|K|})(1-2\delta_{J|J|})(1-2\delta_{m|m|})\overline{A}_{N|K|2} & \\
& \text{IV:} \quad \begin{array}{l} L-J \text{ odd} \\ \ell-m \text{ odd} \end{array}
\end{array} \right.$$

$$\tag{13}$$

where $\overline{A}_{N|K|1}$ and $\overline{A}_{N|K|2}$ are the earth-fixed albedo coefficients of the geophysical spherical harmonics; these harmonics are defined in Appendix 2. Also, I_S, Ω_S, ω_S, and f_S are the orbit parameters for the sun.

Now realizing that any sum of the following sort can be written

$$\sum_{K=-N}^{+N} \sum_{J=-L}^{+L} \sum_{m=-\ell}^{+\ell} C_{KJm} = \sum_{K=0}^{+N} \sum_{J=0}^{+L} \sum_{m=0}^{+\ell} \left[(1+\delta_{oK})(1+\delta_{oJi})(1+\delta_{om})\right]^{-1}$$

$$\cdot \left\{ C_{KJm} + C_{KJ-m} + C_{K-Jm} + C_{K-J-m} + C_{-KJm} + C_{-KJ-m} + C_{-K-Jm} + C_{-K-J-m} \right\}$$

and that

$$(-1)^K = (-1)^{-K} \qquad ,$$

$$\delta_{oj} = \delta_{o-j} \qquad ,$$

as well as making use of (8) - (10) and (13) in (7) yields, after a great deal of labor, the albedo acceleration expressed in terms of the satellite orbit parameters:

$$\ddot{\vec{r}}_L = \frac{\pi R_L^2 C_R F_S^\circ}{c M_L} \left(\frac{a_S}{r_S}\right)^2 \rho^2 \sum_{N=0}^{\infty} \sum_{K=0}^{+N} \sum_{L=0}^{\infty} \sum_{J=0}^{+L} \sum_{\ell=0}^{\infty} \sum_{m=0}^{+\ell}$$

$$\cdot (-1)^K \left[\frac{(2-\delta_{oK})(2N+1)}{(2-\delta_{o1})(2-\delta_{om})(2L+1)(2\ell+1)}\right]^{\frac{1}{2}} \left[1-(-1)^{N+L+\ell}\right] \left[\frac{d_L}{(1+\delta_{oK})(1+\delta_{oJ})(1+\delta_{om})}\right]$$

$$\cdot \sum_{h=0}^{+L} \sum_{p=0}^{+\ell} \overline{F}_{LJh}(I_S) \overline{F}_{\ell mp}(I)$$

$$\cdot \left\{\left[\left[\begin{pmatrix} N & L & \ell-1 \\ 0 & 0 & 0 \end{pmatrix} \left[\left(\frac{b_{\ell-1}}{2\ell-1}\right) - \rho\left(\frac{b_\ell}{2\ell+1}\right)\right] \left[\sqrt{(\ell+m-1)(\ell+m)}\begin{pmatrix} N & L & \ell-1 \\ -K & J & m-1 \end{pmatrix} - \sqrt{(\ell-m-1)(\ell-m)}\begin{pmatrix} N & L & \ell-1 \\ -K & J & m+1 \end{pmatrix}\right]\right]\right.$$

$$- \begin{pmatrix} N & L & \ell+1 \\ 0 & 0 & 0 \end{pmatrix} \left[\left(\frac{b_{\ell+1}}{2\ell+3}\right) - \rho\left(\frac{b_\ell}{2\ell+1}\right)\right] \left[\sqrt{(\ell-m+1)(\ell-m+2)}\begin{pmatrix} N & L & \ell+1 \\ -K & J & m-1 \end{pmatrix} - \sqrt{(\ell+m+1)(\ell+m+2)}\begin{pmatrix} N & L & \ell+1 \\ -K & J & m+1 \end{pmatrix}\right]\right\}$$

14

$$\cdot \begin{cases} \bar{A}_{NK1} \cos(V^S_{LJh} + V^L_{\ell mp} - K\Theta) + \bar{A}_{NK2} \sin(V^S_{LJh} + V^L_{\ell np} - K\Theta) & \text{I} \\[2mm] \bar{A}_{NK1} \sin(V^S_{LJh} + V^L_{\ell mp} - K\Theta) - \bar{A}_{NK2} \cos(V^S_{LJh} + V^L_{\ell mp} - K\Theta) & \text{II} \\[2mm] \bar{A}_{NK1} \sin(V^S_{LJh} + V^L_{\ell mp} - K\Theta) - \bar{A}_{NK2} \cos(V^S_{LJh} + V^L_{\ell mp} - K\Theta) & \text{III} \\[2mm] -\bar{A}_{NK1} \cos(V^S_{LJh} + V^L_{\ell mp} - K\Theta) - \bar{A}_{NK2} \sin(V^S_{LJh} + V^L_{\ell mp} - K\Theta) & \text{IV} \end{cases}$$

$$+(-1)^m \left\{ \begin{pmatrix} N & L & \ell-1 \\ 0 & 0 & 0 \end{pmatrix} \left[\left(\frac{b_\ell}{2\ell-1}\right) - \rho\left(\frac{b_\ell}{2\ell+1}\right) \right] \left[\sqrt{(\ell-m-1)(\ell-m)} \begin{pmatrix} N & L & \ell-1 \\ -K & J & -m-1 \end{pmatrix} - \sqrt{(\ell+m-1)(\ell+m)} \begin{pmatrix} N & L & \ell-1 \\ -K & J & -m+1 \end{pmatrix} \right] \right.$$

$$\left. - \begin{pmatrix} N & L & \ell+1 \\ 0 & 0 & 0 \end{pmatrix} \left[\left(\frac{b_{\ell+1}}{2\ell+3}\right) - \rho\left(\frac{b_\ell}{2\ell+1}\right) \right] \left[\sqrt{(\ell+m+1)(\ell+m+2)} \begin{pmatrix} N & L & \ell+1 \\ -K & J & -m-1 \end{pmatrix} - \sqrt{(\ell-m+1)(\ell-m+2)} \begin{pmatrix} N & L & \ell+1 \\ -K & J & -m+1 \end{pmatrix} \right] \right\}$$

$$\cdot \begin{cases} \bar{A}_{NK1} \cos(V^S_{LJh} - V^L_{\ell mp} - K\Theta) + \bar{A}_{NK2} \sin(V^S_{LJh} - V^L_{\ell mp} - K\Theta) & \text{I} \\[2mm] -\bar{A}_{NK1} \sin(V^S_{LJh} - V^L_{\ell mp} - K\Theta) + \bar{A}_{NK2} \cos(V^S_{LJh} - V^L_{\ell mp} - K\Theta) & \text{II} \\[2mm] \bar{A}_{NK1} \sin(V^S_{LJh} - V^L_{\ell mp} - K\Theta) - \bar{A}_{NK2} \cos(V^S_{LJh} - V^L_{\ell mp} - K\Theta) & \text{III} \\[2mm] \bar{A}_{NK1} \cos(V^S_{LJh} - V^L_{\ell mp} - K\Theta) + \bar{A}_{NK2} \sin(V^S_{LJh} - V^L_{\ell mp} - K\Theta) & \text{IV} \end{cases}$$

$$+(-1)^J \left\{ \begin{pmatrix} N & L & \ell-1 \\ 0 & 0 & 0 \end{pmatrix} \left[\left(\frac{b_{\ell-1}}{2\ell-1}\right) - \rho\left(\frac{b_\ell}{2\ell+1}\right) \right] \left[\sqrt{(\ell+m-1)(\ell+m)} \begin{pmatrix} N & L & \ell-1 \\ -K & -J & m-1 \end{pmatrix} \right. \right.$$

$$\left. \left. - \sqrt{(\ell-m-1)(\ell-m)} \begin{pmatrix} N & L & \ell-1 \\ -K & -J & m+1 \end{pmatrix} \right] \right]$$

$$-\begin{pmatrix} N & L & \ell+1 \\ & & \\ 0 & 0 & 0 \end{pmatrix}\left[\left(\frac{b_{\ell+1}}{2\ell+3}\right)-\rho\left(\frac{b_\ell}{2\ell+1}\right)\right]\left[\sqrt{(\ell-m+1)(\ell-m+2)}\begin{pmatrix} N & L & \ell+1 \\ & & \\ -K & -J & m-1 \end{pmatrix}\right.$$

$$\left.-\sqrt{(\ell+m+1)(\ell+m+2)}\begin{pmatrix} N & L & \ell+1 \\ & & \\ -K & -J & m+1 \end{pmatrix}\right]\Biggr\}$$

$$\cdot\begin{cases} \bar{A}_{NK1}\cos(V^S_{LJh}-V^L_{\ell mp}+K\Theta)-\bar{A}_{NK2}\sin(V^S_{LJh}-V^L_{\ell mp}+K\Theta) & \mathrm{I} \\[8pt] -\bar{A}_{NK1}\sin(V^S_{LJh}-V^L_{\ell mp}+K\Theta)-\bar{A}_{NK2}\cos(V^S_{LJh}-V^L_{\ell mp}+K\Theta) & \mathrm{II} \\[8pt] \bar{A}_{NK1}\sin(V^S_{LJh}-V^L_{\ell mp}+K\Theta)+\bar{A}_{NK2}\cos(V^S_{LJh}-V^L_{\ell mp}+K\Theta) & \mathrm{III} \\[8pt] \bar{A}_{NK_{\bar{1}}}\cos(V^S_{LJh}-V^L_{\ell mp}+K\Theta)-\bar{A}_{NK2}\sin(V^S_{LJh}-V^L_{\ell mp}+K\Theta) & \mathrm{IV} \end{cases}$$

$$+(-1)^{J+m}\Biggl\{\begin{pmatrix} N & L & \ell-1 \\ & & \\ 0 & 0 & 0 \end{pmatrix}\left[\left(\frac{b_{\ell-1}}{2\ell-1}\right)-\rho\left(\frac{b_\ell}{2\ell+1}\right)\right]\left[\sqrt{(\ell-m-1)(\ell-m)}\begin{pmatrix} N & L & \ell-1 \\ & & \\ -K & -J & -m-1 \end{pmatrix}\right.$$

$$\left.-\sqrt{(\ell+m-1)(\ell+m)}\begin{pmatrix} N & L & \ell-1 \\ & & \\ -K & -J & -m+1 \end{pmatrix}\right]$$

$$-\begin{pmatrix} N & L & \ell+1 \\ & & \\ 0 & 0 & 0 \end{pmatrix}\left[\left(\frac{b_{\ell+1}}{2\ell+3}\right)-\rho\left(\frac{b_\ell}{2\ell+1}\right)\right]\left[\sqrt{(\ell+m+1)(\ell+m+2)}\begin{pmatrix} N & L & \ell+1 \\ & & \\ -K & -J & -m-1 \end{pmatrix}\right.$$

$$\left.-\sqrt{(\ell-m+1)(\ell-m+2)}\begin{pmatrix} N & L & \ell+1 \\ & & \\ -K & -J & -m+1 \end{pmatrix}\right]\Biggr\}$$

16

$$\cdot \left\{ \begin{array}{ll} \overline{A}_{NK1} \cos (V^S_{LJh} + V^L_{\ell mp} + K\,\Theta) \; - \; \overline{A}_{NK2} \sin (V^S_{LJh} + V^L_{\ell mp} + K\,\Theta) & I \\[12pt] \overline{A}_{NK1} \sin (V^S_{LJh} + V^L_{\ell mp} + K\,\Theta) \; + \; \overline{A}_{NK2} \cos (V^S_{LJh} + V^L_{\ell mp} + K\,\Theta) & II \\[12pt] \overline{A}_{NK1} \sin (V^S_{LJh} + V^L_{\ell mp} + K\,\Theta) \; + \; \overline{A}_{NK2} \cos (V^S_{LJh} + V^L_{\ell mp} + K\,\Theta) & III \\[12pt] - \overline{A}_{NK1} \cos (V^S_{LJh} + V^L_{\ell mp} + K\,\Theta) \; + \; \overline{A}_{NK2} \sin (V^S_{LJh} + V^L_{\ell mp} + K\,\Theta) & IV \end{array} \right\} \hat{x}$$

$$+ \left[\left\{ \begin{pmatrix} N & L & \ell-1 \\ 0 & 0 & 0 \end{pmatrix} \left[\left(\frac{b_{\ell-1}}{2\ell-1} \right) - \rho \left(\frac{b_\ell}{2\ell+1} \right) \right] \left[\sqrt{(\ell+m-1)(\ell+m)} \begin{pmatrix} N & L & \ell-1 \\ -K & J & m-1 \end{pmatrix} \right] \right. \right.$$

$$\left. + \sqrt{(\ell-m-1)(\ell-m)} \begin{pmatrix} N & L & \ell-1 \\ -K & J & m+1 \end{pmatrix} \right] \Bigg\}$$

$$- \begin{pmatrix} N & L & \ell+1 \\ 0 & 0 & 0 \end{pmatrix} \left[\left(\frac{b_{\ell+1}}{2\ell+3} \right) - \rho \left(\frac{b_\ell}{2\ell+1} \right) \right] \left[\sqrt{(\ell-m+1)(\ell-m+2)} \begin{pmatrix} N & L & \ell+1 \\ -K & J & m-1 \end{pmatrix} \right.$$

$$\left. + \sqrt{(\ell+m+1)(\ell+m+2)} \begin{pmatrix} N & L & \ell+1 \\ -K & J & m+1 \end{pmatrix} \right] \Bigg\}$$

$$\cdot \left\{ \begin{array}{ll} \overline{A}_{NK1} \sin (V^S_{LJh} + V^L_{\ell mp} - K\,\Theta) \; - \; \overline{A}_{NK2} \cos (V^S_{LJh} + V^L_{\ell mp} - K\,\Theta) & I \\[12pt] - \overline{A}_{NK1} \cos (V^S_{LJh} + V^L_{\ell mp} - K\,\Theta) \; - \; \overline{A}_{NK2} \sin (V^S_{LJh} + V^L_{\ell mp} - K\,\Theta) & II \\[12pt] - \overline{A}_{NK1} \cos (V^S_{LJh} + V^L_{\ell mp} - K\,\Theta) \; - \; \overline{A}_{NK2} \sin (V^S_{LJh} + V^L_{\ell mp} - K\,\Theta) & III \\[12pt] - \overline{A}_{NK1} \sin (V^S_{LJH} + V^L_{\ell mp} - K\,\Theta) \; \div \; \overline{A}_{NK2} \cos (V^S_{LJh} + V^L_{\ell mp} - K\,\Theta) & IV \end{array} \right.$$

17

$$+ (-1)^m \left\{ \begin{pmatrix} N & L & \ell-1 \\ & & \\ 0 & 0 & 0 \end{pmatrix} \left[\left(\frac{b_{\ell-1}}{2\ell-1} \right) - \rho \left(\frac{b_\ell}{2\ell+1} \right) \right] \left[\sqrt{(\ell-m-1)(\ell-m)} \begin{pmatrix} N & L & \ell-1 \\ & & \\ -K & J & -m-1 \end{pmatrix} \right. \right.$$

$$\left. + \sqrt{(\ell+m-1)(\ell+m)} \begin{pmatrix} N & L & \ell-1 \\ & & \\ -K & J & -m+1 \end{pmatrix} \right]$$

$$- \begin{pmatrix} N & L & \ell+1 \\ & & \\ 0 & 0 & 0 \end{pmatrix} \left[\left(\frac{b_{\ell+1}}{2\ell+3} \right) - \rho \left(\frac{b_\ell}{2\ell+1} \right) \right] \left[\sqrt{(\ell+m+1)(\ell+m+2)} \begin{pmatrix} N & L & \ell+1 \\ & & \\ -K & J & -m-1 \end{pmatrix} \right.$$

$$\left. \left. + \sqrt{(\ell-m+1)(\ell-m+2)} \begin{pmatrix} N & L & \ell+1 \\ & & \\ -K & J & -m+1 \end{pmatrix} \right] \right\}$$

$$\cdot \begin{cases} \overline{A}_{NK1} \sin (V^S_{LJh} - V^L_{\ell mp} - K\Theta) \quad - \overline{A}_{NK2} \cos (V^S_{LJh} - V^L_{\ell mp} - K\Theta) & \quad \text{I} \\[8pt] \overline{A}_{NK1} \cos (V^S_{LJh} - V^L_{\ell mp} - K\Theta) \quad + \overline{A}_{NK2} \sin (V^S_{LJh} - V^L_{\ell mp} - K\Theta) & \quad \text{II} \\[8pt] -\overline{A}_{NK1} \cos (V^S_{LJh} - V^L_{\ell mp} - K\Theta) \quad - \overline{A}_{NK2} \sin (V^S_{LJh} - V^L_{\ell mp} - K\Theta) & \quad \text{III} \\[8pt] A_{NK1} \sin (V^S_{LJh} - V^L_{\ell mp} - K\Theta) \quad - \overline{A}_{NK2} \cos (V^S_{LJh} - V^L_{\ell mp} - K\Theta) & \quad \text{IV} \end{cases}$$

$$+ (-1)^J \left\{ \begin{pmatrix} N & L & \ell-1 \\ & & \\ 0 & 0 & 0 \end{pmatrix} \left[\left(\frac{b_{\ell-1}}{2\ell-1} \right) - \rho \left(\frac{b_\ell}{2\ell+1} \right) \right] \left[\sqrt{(\ell+m-1)(\ell+m)} \begin{pmatrix} N & L & \ell-1 \\ & & \\ -K & -J & m-1 \end{pmatrix} \right. \right.$$

$$\left. + \sqrt{(\ell-m-1)(\ell-m)} \begin{pmatrix} N & L & \ell-1 \\ & & \\ -K & -J & m+1 \end{pmatrix} \right]$$

$$
- \begin{pmatrix} N & L & \ell+1 \\ & & \\ 0 & 0 & 0 \end{pmatrix} \left[\left(\frac{b_{\ell+1}}{2\ell+3} \right) - \rho \left(\frac{b_\ell}{2\ell+1} \right) \right] \left[\sqrt{(\ell-m+i)(\ell-m+2)} \begin{pmatrix} N & L & \ell+1 \\ & & \\ -K & J & m-1 \end{pmatrix} \right.
$$

$$
\left. \left. + \sqrt{(\ell+m+1)(\ell+m+2)} \begin{pmatrix} N & L & \ell+1 \\ & & \\ -K & -J & m+1 \end{pmatrix} \right] \right\}
$$

$$
\cdot \left\{ \begin{array}{ll}
- \overline{A}_{NK1} \sin(V^S_{LJh} - V^L_{\ell mp} + K\Theta) - \overline{A}_{NK2} \cos(V^S_{LJh} - V^L_{\ell mp} + K\Theta) & \text{I} \\[2mm]
- \overline{A}_{NK1} \cos(V^S_{LJh} - V^L_{\ell mp} + K\Theta) + \overline{A}_{NK2} \sin(V^S_{LJh} - V^L_{\ell mp} + K\Theta) & \text{II} \\[2mm]
+ \overline{A}_{NK1} \cos(V^S_{LJh} - V^L_{\ell mp} + K\Theta) - \overline{A}_{NK2} \sin(V^S_{LJh} - V^L_{\ell mp} + K\Theta) & \text{III} \\[2mm]
- \overline{A}_{NK1} \sin(V^S_{LJh} - V^L_{\ell mp} + K\Theta) - \overline{A}_{NK2} \cos(V^S_{LJh} - V^L_{\ell mp} + K\Theta) & \text{IV}
\end{array} \right.
$$

$$
+ (-1)^{J+m} \left\{ \begin{pmatrix} N & L & \ell-1 \\ & & \\ 0 & 0 & 0 \end{pmatrix} \left[\left(\frac{b_{\ell-1}}{2\ell-1} \right) - \rho \left(\frac{b_\ell}{2\ell+1} \right) \right] \left[\sqrt{(\ell-m-1)(\ell-m)} \begin{pmatrix} N & L & \ell-1 \\ & & \\ -K & -J & -m-1 \end{pmatrix} \right. \right.
$$

$$
\left. + \sqrt{(\ell+m-1)(\ell+m)} \begin{pmatrix} N & L & \ell-1 \\ & & \\ -K & -J & -m+1 \end{pmatrix} \right]
$$

$$
- \begin{pmatrix} N & L & \ell+1 \\ & & \\ 0 & 0 & 0 \end{pmatrix} \left[\left(\frac{b_{\ell+1}}{2\ell+3} \right) - \rho \left(\frac{b_\ell}{2\ell+1} \right) \right] \left[\sqrt{(\ell+m+1)(\ell+m+2)} \begin{pmatrix} N & L & \ell+1 \\ & & \\ -K & -J & -m-1 \end{pmatrix} \right.
$$

$$
\left. \left. + \sqrt{(\ell-m+1)(\ell-m+2)} \begin{pmatrix} N & L & \ell+1 \\ & & \\ -K & -J & -m+1 \end{pmatrix} \right] \right\}
$$

19

$$\cdot \left. \begin{cases} -\bar{A}_{NK1}\sin(V^S_{LJh}+V^L_{\ell mp}+K\Theta) - \bar{A}_{NK2}\cos(V^S_{LJh}+V^L_{\ell mp}+K\Theta) & \text{I} \\ +\bar{A}_{NK1}\cos(V^S_{LJh}+V^L_{\ell mp}+K\Theta) - \bar{A}_{NK2}\sin(V^S_{LJh}+V^L_{\ell mp}+K\Theta) & \text{II} \\ \bar{A}_{NK1}\cos(V^S_{LJh}+V^L_{\ell mp}+K\Theta) - \bar{A}_{NK2}\sin(V^S_{LJh}+V^L_{\ell mp}+K\Theta) & \text{III} \\ \bar{A}_{NK1}\sin(V^S_{LJh}+V^L_{\ell mp}+K\Theta) + \bar{A}_{NK2}\cos(V^S_{LJh}+V^L_{\ell mp}+K\Theta) & \text{IV} \end{cases} \right] \hat{y}$$

$$+2\left[\left\{ \begin{pmatrix} N & L & \ell-1 \\ 0 & 0 & 0 \end{pmatrix} \left[\left(\frac{b_{\ell-1}}{2\ell-1}\right) - \rho\left(\frac{b_\ell}{2\ell+1}\right)\right] \left[\sqrt{(\ell-m)(\ell+m)} \begin{pmatrix} N & L & \ell-1 \\ -K & J & m \end{pmatrix} \right.\right.\right.$$

$$\left.\left.\left. + \begin{pmatrix} N & L & \ell+1 \\ 0 & 0 & 0 \end{pmatrix} \left[\left(\frac{b_{\ell+1}}{2\ell+3}\right) - \rho\left(\frac{b_\ell}{2\ell+1}\right)\right] \left[\sqrt{(\ell-m+1)(\ell+m+1)} \begin{pmatrix} N & L & \ell+1 \\ -K & J & m \end{pmatrix} \right]\right\}\right.$$

$$\cdot \begin{cases} \bar{A}_{NK1}\cos(V^S_{LJh}+V^L_{\ell mp}-K\Theta) + \bar{A}_{NK2}\sin(V^S_{LJh}+V^L_{\ell mp}-K\Theta) & \text{I} \\ \bar{A}_{NK1}\sin(V^S_{LJh}+V^L_{\ell mp}-K\Theta) - \bar{A}_{NK2}\cos(V^S_{LJh}+V^L_{\ell mp}-K\Theta) & \text{II} \\ \bar{A}_{NK1}\sin(V^S_{LJh}+V^L_{\ell mp}-K\Theta) - \bar{A}_{NK2}\cos(V^S_{LJh}+V^L_{\ell mp}-K\Theta) & \text{III} \\ -\bar{A}_{NK1}\cos(V^S_{LJh}+V^L_{\ell mp}-K\Theta) - \bar{A}_{NK2}\sin(V^S_{LJh}+V^L_{\ell mp}-K\Theta) & \text{IV} \end{cases}$$

$$+(-1)^m \left\{ \begin{pmatrix} N & L & \ell-1 \\ 0 & 0 & 0 \end{pmatrix} \left[\left(\frac{b_{\ell-1}}{2\ell-1}\right) - \rho\left(\frac{b_\ell}{2\ell+1}\right)\right] \left[\sqrt{(\ell-m)(\ell+m)} \begin{pmatrix} N & L & \ell-1 \\ -K & J & -m \end{pmatrix}\right] \right.$$

$$\left. + \begin{pmatrix} N & L & \ell+1 \\ 0 & 0 & 0 \end{pmatrix} \left[\left(\frac{b_{\ell+1}}{2\ell+3}\right) - \rho\left(\frac{b_\ell}{2\ell+1}\right)\right] \left[\sqrt{(\ell-m+1)(\ell+m+1)} \begin{pmatrix} N & L & \ell+1 \\ -K & J & -m \end{pmatrix}\right] \right\}$$

$$\cdot \begin{cases} \bar{A}_{NK1} \cos (V^S_{LJh} - V^L_{\ell mp} - K\Theta) + \bar{A}_{NK2} \sin (V^S_{LJh} - V^L_{\ell mp} - K\Theta) & \text{I} \\[6pt] - \bar{A}_{NK1} \sin (V^S_{LJh} - V^L_{\ell mp} - K\Theta) + \bar{A}_{NK2} \cos (V^S_{LJh} - V^L_{\ell mp} - K\Theta) & \text{Ii} \\[6pt] \bar{A}_{NK1} \sin (V^S_{LJh} - V^L_{\ell mp} - K\Theta) - \bar{A}_{NK2} \cos (V^S_{LJh} - V^L_{\ell mp} - K\Theta) & \text{III} \\[6pt] \bar{A}_{NK1} \cos (V^S_{LJh} - V^L_{\ell mp} - K\Theta) + \bar{A}_{NK2} \sin (V^S_{LJh} - V^L_{\ell mp} - K\Theta) & \text{IV} \end{cases}$$

$$+(-1)^J \left\{ \begin{pmatrix} N & L & \ell-1 \\ 0 & 0 & 0 \end{pmatrix} \left[\left(\frac{b_{\ell-1}}{2\ell-1}\right) - \rho \left(\frac{b_\ell}{2\ell+1}\right) \right] \left[\sqrt{(\ell-m)(\ell+m)} \begin{pmatrix} N & L & \ell+1 \\ -K & -J & m \end{pmatrix} \right] \right.$$

$$\left. + \begin{pmatrix} N & L & \ell+1 \\ 0 & 0 & 0 \end{pmatrix} \left[\left(\frac{b_{\ell+1}}{2\ell+3}\right) - \rho \left(\frac{b_\ell}{2\ell+1}\right) \right] \left[\sqrt{(\ell-m+1)(\ell+m+1)} \begin{pmatrix} N & L & \ell+1 \\ -K & -J & m \end{pmatrix} \right] \right\}$$

$$\cdot \begin{cases} \bar{A}_{NK1} \cos (V^S_{LJh} - V^L_{\ell mp} + K\Theta) - \bar{A}_{NK2} \sin (V^S_{LJh} - V^L_{\ell mp} + K\Theta) & \text{i} \\[6pt] - \bar{A}_{NK1} \sin (V^S_{LJh} - V^L_{\ell mp} + K\Theta) - \bar{A}_{NK2} \cos (V^S_{LJh} - V^L_{\ell mp} + K\Theta) & \text{II} \\[6pt] \bar{A}_{NK1} \sin (V^S_{LJh} - V^L_{\ell mp} + K\Theta) + \bar{A}_{NK2} \cos (V^S_{LJh} - V^L_{\ell mp} + K\Theta) & \text{III} \\[6pt] \bar{A}_{NK1} \cos (V^S_{LJh} - V^L_{\ell mp} + K\Theta) - \bar{A}_{NK2} \sin (V^S_{LJh} - V^L_{\ell mp} + K\Theta) & \text{IV} \end{cases}$$

$$+(-1)^{J+m} \left\{ \begin{pmatrix} N & L & \ell-1 \\ 0 & 0 & 0 \end{pmatrix} \left[\left(\frac{b_{\ell-1}}{2\ell-1}\right) - \rho \left(\frac{b_\ell}{2\ell+1}\right) \right] \left[\sqrt{(\ell-m)(\ell+m)} \begin{pmatrix} N & L & \ell-1 \\ -K & -J & -m \end{pmatrix} \right] \right.$$

$$\left. + \begin{pmatrix} N & L & \ell+1 \\ 0 & 0 & 0 \end{pmatrix} \left[\left(\frac{b_{\ell+1}}{2\ell+3}\right) - \rho \left(\frac{b_\ell}{2\ell+1}\right) \right] \left[\sqrt{(\ell-m+1)(\ell+m+1)} \begin{pmatrix} N & L & \ell+1 \\ -K & -J & -m \end{pmatrix} \right] \right\}$$

$$
\cdot \left\{
\begin{array}{ll}
\overline{A}_{NK1} \cos (V_{LJh}^S + V_{\ell mp}^L + K\ \Theta\ ) \ - \ \overline{A}_{NK2} \sin (V_{LJh}^S + V_{\ell mp}^L + K\ \Theta\ ) & \text{I} \\
\overline{A}_{NK1} \sin (V_{LJh}^S + V_{\ell mp}^L + K\ \Theta\ ) \ + \ \overline{A}_{NK2} \cos (V_{LJh}^S + V_{\ell mp}^L + K\ \Theta\ ) & \text{II} \\
\overline{A}_{NK1} \sin (V_{LJh}^S + V_{\ell mp}^L + K\ \Theta\ ) \ + \ \overline{A}_{NK2} \cos (V_{LJh}^S + V_{\ell mp}^L + K\ \Theta\ ) & \text{III} \\
-\overline{A}_{NK1} \cos (V_{LJh}^S + V_{\ell mp}^L + K\ \Theta\ ) \ + \ \overline{A}_{NK2} \sin (V_{LJh}^S + V_{\ell mp}^L + K\ \Theta\ ) & \text{IV}
\end{array}
\right] \hat{z} \right\} \quad (14)
$$

In this equation

$$
V_{LJh}^S = (L - 2h)(\omega_S + f_S) + J\Omega_S
$$

and

$$
V_{\ell mp}^L = (\ell - 2p)(\omega + f) + m\Omega
$$

It should be noted that K, J, and m are now non-negative numbers, as may be seen from the summation symbols in (14). Also, only the Roman numerals for the four conditions are given to save from writing "L – M even, ℓ – m even " etc., over and over.

It is of some interest that the leading subscript on the inclination functions can take on the values 0 and 1, in contrast to the gravitational case. These functions are listed in Table III, since they are not given in the standard references.

The albedo acceleration can be expressed in terms of the orthogonal components (R, S, W) used in Gauss' form of Lagrange's planetary equations. These components are derived via a rotation matrix from the Cartesian components, $(\ddot{x}, \ddot{y}, \ddot{x})$ found in (14):

$$
\begin{bmatrix} R \\ S \\ W \end{bmatrix} =
\begin{bmatrix}
\begin{array}{l} \cos (\omega + f) \cos \Omega \\ -\cos I \sin \Omega \sin (\omega + f) \end{array} &
\begin{array}{l} \cos (\omega + f) \sin \Omega \\ +\cos I \cos \Omega \sin (\omega + f) \end{array} &
\sin (\omega + f) \sin I \\
\begin{array}{l} -\sin (\omega + f) \cos \Omega \\ -\cos I \sin \Omega \cos (\omega + f) \end{array} &
\begin{array}{l} -\sin (\omega + f) \sin \Omega \\ +\cos I \cos \Omega \cos (\omega + f) \end{array} &
\cos (\omega + f) \sin I \\
\sin I \sin \Omega & -\sin I \cos\Omega & \cos I
\end{bmatrix}
\begin{bmatrix} \ddot{x} \\ \ddot{y} \\ \ddot{z} \end{bmatrix} \quad (15)
$$

(Rubincam, 1982, p. 370). In this equation R is the radial component of acceleration, S is the transverse component in the plane of the orbit, perpendicular to R and positive in the direction of motion, while W is normal to the orbital plane and positive in the direction of the angular momentum (e.g., Blanco and McCuskey, 1961, pp. 177-178). Of course $\ddot{\vec{r}}_L = \ddot{x}\,\hat{x} + \ddot{y}\,\hat{y} + \ddot{z}\,\hat{z}$.

The general equations for R, S, and W will not be written here. Instead only the case of zonal albedo variations will be considered, so that the light and dark markings of the earth vary only with latitude. The reason for doing this is that only the zonals will give a long-term change in the Keplerian elements, barring a resonance. So $K = 0$ from this point onward.

Using the general relations

$$
\begin{aligned}
\cos a \cos b &= \tfrac{1}{2}\cos(a+b) + \tfrac{1}{2}\cos(a-b) \\
\sin a \sin b &= -\tfrac{1}{2}\cos(a+b) + \tfrac{1}{2}\cos(a-b) \\
\sin a \cos b &= \tfrac{1}{2}\sin(a+b) + \tfrac{1}{2}\sin(a-b) \\
\cos a \sin b &= \tfrac{1}{2}\sin(a+b) - \tfrac{1}{2}\sin(a-b)
\end{aligned}
\tag{16}
$$

(e.g., Kaula, 1966, p.31) together with (14) and (15) yields the following equation for the radial albedo acceleration:

$$
R = \frac{\pi R_L^2 C_R F_S^{\,\circ}}{4 c M_L} \left(\frac{a_S}{r_S}\right)^2 \rho^2 \sum_{N=0}^{\infty} \sum_{L=0}^{\infty} \sum_{J=0}^{+L} \sum_{\ell=0}^{\infty} \sum_{m=0}^{+\ell} \; {}_d\!{}_L \bar{A}_{N01}
$$

$$
\cdot \left[\frac{(2N+1)}{(2-\delta_{oJ})(2-\delta_{om})(2L+1)(2\ell+1)}\right]^{1/2} \frac{[1-(-1)^{N+L+\ell}]^2}{(1+\delta_{oJ})(1+\delta_{om})} \sum_{h=0}^{+L} \sum_{p=0}^{+\ell} \bar{F}_{LJh}(I_S)\, \bar{F}_{\ell m p}(I)
$$

$$
\cdot \left[\left\{ \sqrt{(\ell-m+1)(\ell-m+2)} \left[\left(\frac{b_{\ell+1}}{2\ell+3}\right) - \rho\left(\frac{b_\ell}{2\ell+1}\right)\right] \begin{pmatrix} N & L & \ell+1 \\ 0 & 0 & 0 \end{pmatrix} \begin{pmatrix} N & L & \ell+1 \\ 0 & J & m-1 \end{pmatrix} \right.\right.
$$

$$
\left.\left. - \sqrt{(\ell+m-1)(\ell+m)} \left[\left(\frac{b_{\ell-1}}{2\ell-1}\right) - \rho\left(\frac{b_\ell}{2\ell+1}\right)\right] \begin{pmatrix} N & L & \ell-1 \\ 0 & 0 & 0 \end{pmatrix} \begin{pmatrix} N & L & \ell-1 \\ 0 & J & m-1 \end{pmatrix} \right\} \{1+\cos I\}\right.
$$

$$
\cdot \left\{
\begin{aligned}
& -\cos[V_{LJh}^S + V_{\ell mp}^L - (\omega+f+\Omega)] && \text{I} \\
& -\sin[V_{LJh}^S + V_{\ell mp}^J - (\omega+f+\Omega)] && \text{II} \\
& -\sin[V_{LJh}^S + V_{\ell mp}^L - (\omega+f+\Omega)] && \text{III} \\
& +\cos[V_{LJh}^S + V_{\ell mp}^L - (\omega+f+\Omega)] && \text{IV}
\end{aligned}
\right.
$$

23

$$+\left\{\sqrt{(\ell-m+1)(\ell-m+2)}\left[\left(\frac{b_{\ell+1}}{2\ell+3}\right)-\rho\left(\frac{b_\ell}{2\ell+1}\right)\right]\begin{pmatrix}N & L & \ell+1\\ 0 & 0 & 0\end{pmatrix}\begin{pmatrix}N & L & \ell+1\\ 0 & J & m-1\end{pmatrix}\right.$$

$$\left.-\sqrt{(\ell+m-1)(\ell+m)}\left[\left(\frac{b_{\ell-1}}{2\ell-1}\right)-\rho\left(\frac{b_\ell}{2\ell+1}\right)\right]\begin{pmatrix}N & L & \ell-1\\ 0 & 0 & 0\end{pmatrix}\begin{pmatrix}N & L & \ell-1\\ 0 & J & m-1\end{pmatrix}\right\}\left\{1-\cos I\right\}$$

$$\cdot\begin{cases}-\cos\left[V^S_{LJh}+V^S_{\ell mp}+(\omega+f-\Omega)\right] & \text{I}\\ -\sin\left[V^S_{LJh}+V^S_{\ell mp}+(\omega+f-\Omega)\right] & \text{II}\\ -\sin\left[V^S_{LJh}+V^L_{\ell mp}+(\omega+f-\Omega)\right] & \text{III}\\ +\cos\left[V^S_{LJh}+V^L_{\ell mp}+(\omega+f-\Omega)\right] & \text{IV}\end{cases}$$

$$+\left\{\sqrt{(\ell+m+1)(\ell+m+2)}\left[\left(\frac{b_{\ell+1}}{2\ell+3}\right)-\rho\left(\frac{b_\ell}{2\ell+1}\right)\right]\begin{pmatrix}N & L & \ell+1\\ 0 & 0 & 0\end{pmatrix}\begin{pmatrix}N & L & \ell+1\\ 0 & J & m+1\end{pmatrix}\right.$$

$$\left.-\sqrt{(\ell-m-1)(\ell-m)}\left[\left(\frac{b_{\ell-1}}{2\ell-1}\right)-\rho\left(\frac{b_\ell}{2\ell+1}\right)\right]\begin{pmatrix}N & L & \ell-1\\ 0 & 0 & 0\end{pmatrix}\begin{pmatrix}N & L & \ell-1\\ 0 & J & m+1\end{pmatrix}\right\}\left\{1-\cos I\right\}$$

$$\cdot\begin{cases}+\cos\left[V^S_{LJh}+V^L_{\ell mp}-(\omega+f-\Omega)\right] & \text{I}\\ +\sin\left[V^S_{LJh}+V^L_{mp}-(\omega+f-\Omega)\right] & \text{II}\\ +\sin\left[V^S_{LJh}+V^L_{\ell mp}-(\omega+f-\Omega)\right] & \text{III}\\ -\cos\left[V^S_{LJh}+V^L_{\ell mp}-(\omega+f-\Omega)\right] & \text{IV}\end{cases}$$

$$+\left\{\sqrt{(\ell+m+1)(\ell+m+2)}\left[\left(\frac{b_{\ell+1}}{2\ell+3}\right)-\rho\left(\frac{b_\ell}{2\ell+1}\right)\right]\begin{pmatrix}N & L & \ell+1\\ 0 & 0 & 0\end{pmatrix}\begin{pmatrix}N & L & \ell+1\\ 0 & J & m+1\end{pmatrix}\right.$$

$$\left.-\sqrt{(\ell-m-1)(\ell-m)}\left[\left(\frac{b_{\ell-1}}{2\ell-1}\right)-\rho\left(\frac{b_\ell}{2\ell+1}\right)\right]\begin{pmatrix}N & L & \ell-1\\ 0 & 0 & 0\end{pmatrix}\begin{pmatrix}N & L & \ell-1\\ 0 & J & m+1\end{pmatrix}\right\}\left\{1+\cos I\right\}$$

$$\cdot \begin{cases} + \cos\,[V_{LJh}^{S} + V_{\ell mp}^{L} + (\omega + f + \Omega)] & \quad \text{I} \\[4pt] + \sin\,[V_{LJh}^{S} + V_{\ell mp}^{L} + (\omega + f + \Omega)] & \quad \text{II} \\[4pt] + \sin\,[V_{LJh}^{S} + V_{\ell mp}^{L} + (\omega + f + \Omega)] & \quad \text{III} \\[4pt] - \cos\,[V_{LJh}^{S} + V_{\ell mp}^{L} + (\omega + f + \Omega)] & \quad \text{IV} \end{cases}$$

$$+ (-1)^{m}\Bigg\{ \sqrt{(\ell+m+1)(\ell+m+2)}\left[\left(\frac{b_{\ell+1}}{2\ell+3}\right) - \rho\left(\frac{b_{\ell}}{2\ell+1}\right)\right] \begin{pmatrix} N & L & \ell+1 \\ 0 & 0 & 0 \end{pmatrix} \begin{pmatrix} N & L & \ell+1 \\ 0 & J & -m-1 \end{pmatrix}$$

$$- \sqrt{(\ell-m-1)(\ell-m)}\left[\left(\frac{b_{\ell-1}}{2\ell-1}\right) - \rho\left(\frac{b_{\ell}}{2\ell+1}\right)\right] \begin{pmatrix} N & L & \ell-1 \\ 0 & 0 & 0 \end{pmatrix} \begin{pmatrix} N & L & \ell-1 \\ 0 & J & -m-1 \end{pmatrix} \Bigg\} \{1 - \cos I\}$$

$$\cdot \begin{cases} - \cos\,[V_{LJh}^{S} - V_{\ell mp}^{L} + (\omega + f - \Omega)] & \quad \text{I} \\[4pt] + \sin\,[V_{LJh}^{S} - V_{\ell mp}^{L} + (\omega + f - \Omega)] & \quad \text{II} \\[4pt] - \sin\,[V_{LJh}^{S} - V_{\ell mp}^{L} + (\omega + f - \Omega)] & \quad \text{III} \\[4pt] - \cos\,[V_{LJh}^{S} - V_{\ell mp}^{L} + (\omega + f - \Omega)] & \quad \text{IV} \end{cases}$$

$$+ (-1)^{m}\Bigg\{ \sqrt{(\ell+m+1)(\ell+m+2)}\left[\left(\frac{b_{\ell+1}}{2\ell+3}\right) - \rho\left(\frac{b_{\ell}}{2\ell+1}\right)\right] \begin{pmatrix} N & L & \ell+1 \\ 0 & 0 & 0 \end{pmatrix} \begin{pmatrix} N & L & \ell+1 \\ 0 & J & -m-i \end{pmatrix}$$

$$- \sqrt{(\ell-m-1)(\ell-m)}\left[\left(\frac{b_{\ell-1}}{2\ell-i}\right) - \rho\left(\frac{b_{\ell}}{2\ell+1}\right)\right] \begin{pmatrix} N & L & \ell-1 \\ 0 & 0 & 0 \end{pmatrix} \begin{pmatrix} N & L & \ell-1 \\ 0 & J & -m-1 \end{pmatrix} \Bigg\} \{1 + \cos I\}$$

$$\cdot \begin{cases} - \cos\,[V_{LJh}^{S} - V_{\ell mp}^{L} - (\omega + f + \Omega)] & \quad \text{I} \\[4pt] + \sin\,[V_{LJh}^{S} - V_{\ell mp}^{L} - (\omega + f + \Omega)] & \quad \text{II} \\[4pt] - \sin\,[V_{LJh}^{S} - V_{\ell mp}^{L} - (\omega + f + \Omega)] & \quad \text{III} \\[4pt] - \cos\,[V_{LJh}^{S} - V_{\ell mp}^{L} - (\omega + f + \Omega)] & \quad \text{IV} \end{cases}$$

25

$$+(-1)^m\left\{\sqrt{(\ell-m+1)(\ell-m+2)}\left[\left(\frac{b_{\ell+1}}{2\ell+3}\right)-\rho\left(\frac{b_\ell}{2\ell+1}\right)\right]\begin{pmatrix}N & L & \ell+1\\ & & \\0 & 0 & 0\end{pmatrix}\begin{pmatrix}N & L & \ell+1\\ & & \\0 & J & -m+1\end{pmatrix}\right.$$

$$\left.-\sqrt{(\ell+m-1)(\ell+m)}\left[\left(\frac{b_{\ell-1}}{2\ell-1}\right)-\rho\left(\frac{b_\ell}{2\ell+1}\right)\right]\begin{pmatrix}N & L & \ell-1\\ & & \\0 & 0 & 0\end{pmatrix}\begin{pmatrix}N & L & \ell-1\\ & & \\0 & J & -m+1\end{pmatrix}\right\}\left\{1+\cos I\right\}$$

$$\cdot\begin{cases}+\cos\,[V^S_{LJh}-V^L_{\ell mp}+(\omega+f+\Omega)] & \text{I}\\[1em]-\sin\,[V^S_{LJh}-V^L_{\ell mp}+(\omega+f+\Omega)] & \text{II}\\[1em]+\sin\,[V^S_{LJh}-V^L_{\ell mp}+(\omega+f+\Omega)] & \text{III}\\[1em]+\cos\,[V^S_{LJh}-V^L_{\ell mp}+(\omega+f+\Omega)] & \text{IV}\end{cases}$$

$$+(-1)^m\left\{\sqrt{(\ell-m+1)(\ell-m+2)}\left[\left(\frac{b_{\ell+1}}{2\ell+3}\right)-\rho\left(\frac{b_\ell}{2\ell+1}\right)\right]\begin{pmatrix}N & L & \ell+1\\ & & \\0 & 0 & 0\end{pmatrix}\begin{pmatrix}N & L & \ell+1\\ & & \\0 & J & -m+1\end{pmatrix}\right.$$

$$\left.-\sqrt{(\ell+m-1)(\ell+m)}\left[\left(\frac{b_{\ell-1}}{2\ell-1}\right)-\rho\left(\frac{b_\ell}{2\ell+1}\right)\right]\begin{pmatrix}N & L & \ell-1\\ & & \\0 & 0 & 0\end{pmatrix}\begin{pmatrix}N & L & \ell-1\\ & & \\0 & J & -m+1\end{pmatrix}\right\}\left\{1-\cos I\right\}$$

$$\cdot\begin{cases}+\cos\,[V^S_{LJh}-V^L_{\ell mp}-(\omega+f-\Omega)] & \text{I}\\[1em]-\sin\,[V^S_{LJh}-V^L_{\ell mp}-(\omega+f-\Omega)] & \text{II}\\[1em]+\sin\,[V^S_{LJh}-V^L_{\ell mp}-(\omega+f-\Omega)] & \text{III}\\[1em]+\cos\,[V^S_{LJh}-V^L_{\ell mp}-(\omega+f-\Omega)] & \text{IV}\end{cases}$$

$$+2\left\{\sqrt{(\ell-m+1)(\ell+m+1)}\left[\left(\frac{b_{\ell+1}}{2\ell+3}\right)-\rho\left(\frac{b_\ell}{2\ell+1}\right)\right]\begin{pmatrix}N & L & \ell+1\\ 0 & 0 & 0\end{pmatrix}\begin{pmatrix}N & L & \ell+1\\ 0 & J & m\end{pmatrix}\right.$$

$$+\sqrt{(\ell-m)(\ell+m)}\left[\left(\frac{b_{\ell-1}}{2\ell-1}\right)-\rho\left(\frac{b_\ell}{2\ell+1}\right)\right]\begin{pmatrix}N & L & \ell-1\\ 0 & 0 & 0\end{pmatrix}\left.\begin{pmatrix}N & L & \ell-1\\ 0 & J & m\end{pmatrix}\right\}\left\{\sin I\right\}$$

$$\cdot\begin{cases}-\sin[V_{LJh}^S+V_{\ell mp}^L-(\omega+f)] & \text{I}\\ +\cos[V_{LJh}^S+V_{\ell mp}^L-(\omega+f)] & \text{II}\\ +\cos[V_{LJh}^S+V_{\ell mp}^L-(\omega+f)] & \text{III}\\ +\sin[V_{LJh}^S+V_{\ell mp}^L-(\omega+f)] & \text{IV}\end{cases}$$

$$+2\left\{\sqrt{(\ell-m+1)(\ell+m+1)}\left[\left(\frac{b_{\ell+1}}{2\ell+3}\right)-\rho\left(\frac{b_\ell}{2\ell+1}\right)\right]\begin{pmatrix}N & L & \ell+1\\ 0 & 0 & 0\end{pmatrix}\begin{pmatrix}N & L & \ell+1\\ 0 & J & m\end{pmatrix}\right.$$

$$+\sqrt{(\ell-m)(\ell+m)}\left[\left(\frac{b_{\ell-1}}{2\ell-1}\right)-\rho\left(\frac{b}{2\ell+1}\right)\right]\begin{pmatrix}N & L & \ell-1\\ 0 & 0 & 0\end{pmatrix}\left.\begin{pmatrix}N & L & \ell-1\\ 0 & J & m\end{pmatrix}\right\}\left\{\sin I\right\}$$

$$\cdot\begin{cases}+\sin[V_{LJh}^S+V_{\ell mp}^L+(\omega+f)] & \text{I}\\ -\cos[V_{LJh}^S+V_{\ell mp}^L+(\omega+f)] & \text{II}\\ -\cos[V_{LJh}^S+V_{\ell mp}^L+(\omega+f)] & \text{III}\\ -\sin[V_{LJh}^S+V_{\ell mp}^L+(\omega+f)] & \text{IV}\end{cases}$$

$$+2(-1)^m\left\{\sqrt{(\ell-m+1)(\ell+m+1)}\left[\left(\frac{b_{\ell+1}}{2\ell+3}\right)-\rho\left(\frac{b_\ell}{2\ell+1}\right)\right]\begin{pmatrix}N & L & \ell+1\\ 0 & 0 & 0\end{pmatrix}\begin{pmatrix}N & L & \ell+1\\ 0 & J & -m\end{pmatrix}\right.$$

$$+\sqrt{(\ell-m)(\ell+m)}\left[\left(\frac{b_{\ell-1}}{2\ell-1}\right)-\rho\left(\frac{b_\ell}{2\ell+1}\right)\right]\begin{pmatrix}N & L & \ell-1\\ 0 & 0 & 0\end{pmatrix}\left.\begin{pmatrix}N & L & \ell-1\\ 0 & J & -m\end{pmatrix}\right\}\left\{\sin I\right\}$$

27

$$\cdot \begin{cases} -\sin\,[V_{LJh}^{S} \;-\; V_{\ell mp}^{L} \;-\; (\omega + f)] & \text{I} \\[4pt] -\cos[V_{LJh}^{S} \;-\; V_{\ell mp}^{L} \;-\; (\omega + f)] & \text{II} \\[4pt] +\cos[V_{LJh}^{S} \;-\; V_{\ell mp}^{L} \;-\; (\omega + f)] & \text{III} \\[4pt] -\sin\,[V_{LJh}^{S} \;-\; V_{\ell mp}^{L} \;-\; (\omega + f)] & \text{IV} \end{cases}$$

$$+2(-1)^m \left\{ \sqrt{(\ell-m+1)(\ell+m+1)} \left[\left(\frac{b_{\ell+1}}{2\ell+3}\right) - \rho\left(\frac{b_\ell}{2\ell+1}\right) \right] \begin{pmatrix} N & L & \ell+1 \\ 0 & 0 & 0 \end{pmatrix} \begin{pmatrix} N & L & \ell+1 \\ 0 & J & -m \end{pmatrix} \right.$$

$$\left. +\sqrt{(\ell-m)(\ell+m)} \left[\left(\frac{b_{\ell-1}}{2\ell-1}\right) - \rho\left(\frac{b_\ell}{2\ell+1}\right) \right] \begin{pmatrix} N & L & \ell-1 \\ 0 & 0 & 0 \end{pmatrix} \begin{pmatrix} N & L & \ell-1 \\ 0 & J & -m \end{pmatrix} \right\} \quad \left\{ \sin \text{I} \right\}$$

$$\cdot \begin{cases} +\sin\,[V_{LJh}^{S} - V_{\ell mp}^{L} + (\omega + f)] & \text{I} \\[4pt] +\cos[V_{LJh}^{S} - V_{\ell mp}^{L} + (\omega + f)] & \text{II} \\[4pt] -\cos[V_{LJh}^{S} - V_{\ell mp}^{L} + (\omega + f)] & \text{III} \\[4pt] +\sin\,[V_{LJh}^{S} - V_{\ell mp}^{L} + (\omega + f)] & \text{IV} \end{cases} \tag{17}$$

S can be found from (17) by substituting $\omega + f + \pi/2$ for $\omega + f$ where it explicitly appears in the above equation. (The $\omega + f$ hidden in $V_{\ell mp}^{L}$ is not to be tampered with.) Hence S will not be written here.

W is more easily found than R. By (14) and (15) it is

$$W = \frac{\pi R_L^2 C_R F_S^{\circ}}{2cM_L} \left(\frac{a_S}{r_S}\right)^2 \rho^2 \sum_{N=0}^{\infty} \sum_{L=0}^{\infty} \sum_{J=0}^{+L} \sum_{\ell=0}^{\infty} \sum_{m=0}^{+\ell} d_L \overline{A}_{N01}$$

$$\cdot \left[\frac{(2N+1)}{(2-\delta_{oJ})(2-\delta_{om})(2L+1)(2\ell+1)}\right]^{\frac{1}{2}} \left[\frac{1-(-1)^{N+L+\ell}}{(1+\delta_{oJ})(1+\delta_{om})}\right]^2 \sum_{h=0}^{+L} \sum_{p=0}^{+\ell} \overline{F}_{LJh}(I_S)\,\overline{F}_{\ell mp}(I)$$

$$\left[\left\{\sqrt{(\ell+m-1)(\ell+m)}\left[\left(\frac{b_{\ell}-1}{2\ell-1}\right)-\rho\left(\frac{b_{\ell}}{2\ell+1}\right)\right]\begin{pmatrix}N & L & \ell-1\\ 0 & 0 & 0\end{pmatrix}\begin{pmatrix}N & L & \ell-1\\ 0 & J & m-1\end{pmatrix}\right.\right.$$

$$\left.\left.-\sqrt{(\ell-m+1)(\ell-m+2)}\left[\left(\frac{b_{\ell}+1}{2\ell+3}\right)-\rho\left(\frac{b_{\ell}}{2\ell+1}\right)\right]\begin{pmatrix}N & L & \ell+1\\ 0 & 0 & 0\end{pmatrix}\begin{pmatrix}N & L & \ell+1\\ 0 & J & m-1\end{pmatrix}\right\}\left\{\sin I\right\}\right]$$

$$\cdot\left\{\begin{array}{ll}-\sin(V^S_{LJh}+V^L_{\ell mp}-\Omega) & \text{I}\\ +\cos(V^S_{LJh}+V^L_{\ell mp}-\Omega) & \text{II}\\ +\cos(V^S_{LJh}+V^L_{\ell mp}-\Omega) & \text{III}\\ +\sin(V^S_{LJh}+V^L_{\ell mp}-\Omega) & \text{IV}\end{array}\right.$$

$$+\left\{\sqrt{(\ell-m-1)(\ell-m)}\left[\left(\frac{b_{\ell}-1}{2\ell-1}\right)-\rho\left(\frac{b_{\ell}}{2\ell+1}\right)\right]\begin{pmatrix}N & L & \ell-1\\ 0 & 0 & 0\end{pmatrix}\begin{pmatrix}N & L & \ell-1\\ 0 & J & m+1\end{pmatrix}\right.$$

$$\left.-\sqrt{(\ell+m+1)(\ell+m+2)}\left[\left(\frac{b_{\ell}+1}{2\ell+3}\right)-\rho\left(\frac{b_{\ell}}{2\ell+1}\right)\right]\begin{pmatrix}N & L & \ell+1\\ 0 & 0 & 0\end{pmatrix}\begin{pmatrix}N & L & \ell+1\\ 0 & J & m+1\end{pmatrix}\right\}\left\{\sin I\right\}$$

$$\cdot\left\{\begin{array}{ll}-\sin(V^S_{LJh}+V^L_{\ell mp}+\Omega) & \text{I}\\ +\cos(V^S_{LJh}+V^L_{\ell mp}+\Omega) & \text{II}\\ +\cos(V^S_{LJh}+V^L_{\ell mp}+\Omega) & \text{III}\\ +\sin(V^S_{LJh}+V^L_{\ell mp}+\Omega) & \text{IV}\end{array}\right.$$

$$+(-1)^m\left\{\sqrt{(\ell-m-1)(\ell-m)}\left[\left(\frac{b_{\ell}-1}{2\ell-1}\right)-\rho\left(\frac{b_{\ell}}{2\ell+1}\right)\right]\begin{pmatrix}N & L & \ell-1\\ 0 & 0 & 0\end{pmatrix}\begin{pmatrix}N & L & \ell-1\\ 0 & J & -m-1\end{pmatrix}\right.$$

$$\left.-\sqrt{(\ell+m+1)(\ell+m+2)}\left[\left(\frac{b_{\ell}+1}{2\ell+3}\right)-\rho\left(\frac{b_{\ell}}{2\ell+1}\right)\right]\begin{pmatrix}N & L & \ell+1\\ 0 & 0 & 0\end{pmatrix}\begin{pmatrix}N & L & \ell+1\\ 0 & J & -m-1\end{pmatrix}\right\}\left\{\sin I\right\}$$

$$\cdot \begin{cases} -\sin \left(V_{LJh}^{S} - V_{\ell mp}^{L} - \Omega \right) & \text{I} \\ -\cos \left(V_{LJh}^{S} - V_{\ell mp}^{L} - \Omega \right) & \text{II} \\ +\cos \left(V_{LJh}^{S} - V_{\ell mp}^{L} - \Omega \right) & \text{III} \\ -\sin \left(V_{LJh}^{S} - V_{\ell mp}^{L} - \Omega \right) & \text{IV} \end{cases}$$

$$+(-1)^{m} \left\{ \sqrt{(\ell+m-1)(\ell+m)} \left[\left(\frac{b_{\ell-1}}{2\ell-1} \right) - \rho \left(\frac{b_{\ell}}{2\ell+1} \right) \right] \begin{pmatrix} N & L & \ell-1 \\ 0 & 0 & 0 \end{pmatrix} \begin{pmatrix} N & L & \ell-1 \\ 0 & J & -m+1 \end{pmatrix} \right.$$

$$\left. - \sqrt{(\ell-m+1)(\ell-m+2)} \left[\left(\frac{b_{\ell+1}}{2\ell+3} \right) - \rho \left(\frac{b_{\ell}}{2\ell+1} \right) \right] \begin{pmatrix} N & L & \ell+1 \\ 0 & 0 & 0 \end{pmatrix} \begin{pmatrix} N & L & \ell+1 \\ 0 & J & -m+1 \end{pmatrix} \right\} \left\{ \sin I \right\}$$

$$\cdot \begin{cases} -\sin \left(V_{LJh}^{S} - V_{\ell mp}^{L} + \Omega \right) & \text{I} \\ -\cos \left(V_{LJh}^{S} - V_{\ell mp}^{L} + \Omega \right) & \text{II} \\ +\cos \left(V_{LJh}^{S} - V_{\ell mp}^{L} + \Omega \right) & \text{III} \\ -\sin \left(V_{LJh}^{S} - V_{\ell mp}^{L} + \Omega \right) & \text{IV} \end{cases}$$

$$+2 \left\{ \sqrt{(\ell-m)(\ell+m)} \left[\left(\frac{b_{\ell-1}}{2\ell-1} \right) - \rho \left(\frac{b_{\ell}}{2\ell+1} \right) \right] \left[\begin{pmatrix} N & L & \ell-1 \\ 0 & 0 & 0 \end{pmatrix} \begin{pmatrix} N & L & \ell-1 \\ 0 & J & m \end{pmatrix} \right] \right.$$

$$\left. + \sqrt{(\ell-m+1)(\ell+m+1)} \left[\left(\frac{b_{\ell+1}}{2\ell+3} \right) - \rho \left(\frac{b_{\ell}}{2\ell+1} \right) \right] \left[\begin{pmatrix} N & L & \ell+1 \\ 0 & 0 & 0 \end{pmatrix} \begin{pmatrix} N & L & \ell+1 \\ 0 & J & m \end{pmatrix} \right] \right\} \left\{ \cos I \right\}$$

$$\cdot \begin{cases} +\cos \left(V_{LJh}^{S} + V_{\ell mp}^{L} \right) & \text{I} \\ +\sin \left(V_{LJh}^{S} + V_{\ell mp}^{L} \right) & \text{II} \\ +\sin \left(V_{LJh}^{S} + V_{\ell mp}^{L} \right) & \text{III} \\ -\cos \left(V_{LJh}^{S} + V_{\ell mp}^{L} \right) & \text{IV} \end{cases}$$

30

$$+2(-1)^m \left\{ \sqrt{(\ell-m)(\ell+m)} \quad \left[\left(\frac{b_{\ell-1}}{2\ell-1} \right) - \rho \left(\frac{b_\ell}{2\ell+1} \right) \right] \left[\begin{pmatrix} N & L & \ell-1 \\ 0 & 0 & 0 \end{pmatrix} \begin{pmatrix} N & L & \ell-1 \\ 0 & J & -m \end{pmatrix} \right] \right.$$

$$\left. + \sqrt{(\ell-m+1)(\ell+m+1)} \left[\left(\frac{b_{\ell+1}}{2\ell+3} \right) - \rho \left(\frac{b_\ell}{2\ell+1} \right) \right] \left[\begin{pmatrix} N & L & \ell+1 \\ 0 & 0 & 0 \end{pmatrix} \begin{pmatrix} N & L & \ell+1 \\ 0 & J & -m \end{pmatrix} \right] \right\} \left\{ \cos I \right\}$$

$$\cdot \left\{ \begin{array}{ll} +\cos (V^S_{LJh} - V^L_{\ell mp}) & \text{I} \\ -\sin (V^S_{LJh} - V^L_{\ell mp}) & \text{II} \\ +\sin (V^S_{LJh} - V^L_{\ell mp}) & \text{III} \\ +\cos (V^S_{LJh} - V^L_{\ell mp}) & \text{IV} \end{array} \right] \qquad (18)$$

Again it is to be reminded that (17) and (18) apply only to zonal variations in albedo, i.e., $K = 0$ in these equations.

This completes the lengthy derivation of the albedo acceleration. It remains to find the d_L and b_ℓ.

3. Derivation of coefficients

The d_L will be found first. Define a "hemisphere function" H such that

$$H = \left\{ \begin{array}{ll} 1 & \text{in the sunlit hemisphere} \\ \\ 0 & \text{elsewhere} \end{array} \right. \quad ;$$

then H has the Legendre polynomial expansion

$$H = \sum_{L=0}^{\infty} H_L P_L (\cos \psi_S)$$

where

$$H_L = \tfrac{1}{2} [P_{L-1} (0) - P_{L+1} (0)]$$

with

$$P_{-1} (0) \equiv +1$$

31

(Longman, 1962, pp. 846-847). Defining now the "daylight function"

$$D = H \cos \psi_S = \sum_{L=0}^{\infty} H_L \cos \psi_S P_L (\cos \psi_S)$$

insures the proper behavior of the irradiance over the whole earth: $\sim \cos \psi_S$ in the sunlit hemisphere, ~ 0 in the shadowed. Using

$$P_L (\cos \psi_S) = \frac{(L+1) P_{L+1}(\cos \psi_S) + L P_{L-1}(\cos \psi_S)}{(2L+1)}$$

(Hobson, 1955, p. 32) allows writing

$$D = \sum_{L=0}^{\infty} d_L P_L (\cos \psi_S)$$

as required, where

$$d_L = \left(\frac{L}{2L-1}\right) H_{L-1} + \left(\frac{L+1}{2L+3}\right) H_{L+1}$$

$$= \frac{1}{2} \left[-\left(\frac{L+1}{2L+3}\right) P_{L+2}(0) - \frac{(2L+1)}{(2L-1)(2L+3)} P_L(0) + \left(\frac{L}{2L-1}\right) P_{L-2}(0) \right]$$

and $P_{-2}(0) \equiv 0$.

The d_L can now be found from standard tables for the Legendre polynomials (e.g., Hobson, 1955, p. 17). A listing of the d_L for $0 \leqslant L \leqslant 6$ is given in Table IV. Note that all of the d_L for odd L are zero, except for d_1. A graph of D using the first seven terms in the summation is shown in Figure 4. Notice that it is an excellent approximation to the exact function.

Finding the b_ϱ is harder work. Using the binomial expansion (e.g., Selby, 1973, p. 470)

$$(1 - 2\rho \cos \eta + \rho)^{-2} = (1 + q)^{-2} = 1 - 2q + 3q^2 - 4q^3 \div \ldots$$

(where $q = -2\rho \cos \eta + \rho^2$) and multiplying $\cos \eta - \rho$ gives the following approximation B' for B:

$$\mathbf{B'} = (\cos\eta - \rho)\ (1 - 2q + 3q^2 - \ldots)$$

$$\approx (-\rho + 2\rho^3 - 3\rho^5 + 4\rho^7 - 5\rho^9 + 6\rho^{11} - 7\rho^{13} + 8\rho^{15} - 9\rho^{17} + 10\rho^{19} - 11\rho^{21} + 12\rho^{23}$$

$$- 13\rho^{25} + 14\rho^{27} - 15\rho^{29} + 16\rho^{31})$$

$$+ (1 - 6\rho^2 + 15\rho^4 - 28\rho^6 + 45\rho^8 - 66\rho^{10} + 91\rho^{12} - 120\rho^{14} + 153\rho^{16} - 190\rho^{18} + 231\rho^{20}$$

$$- 276\rho^{22} + 325\rho^{24} - 378\rho^{26} + 435\rho^{28} - 496\rho^{30})\cos\eta$$

$$+ (4\rho - 24\rho^3 + 72\rho^5 - 160\rho^7 + 300\rho^9 - 504\rho^{11} + 784\rho^{13} - 1152\rho^{15} + 1620\rho^{17} - 2200\rho^{19}$$

$$+ 2904\rho^{21} - 3744\rho^{23} + 4732\rho^{25} - 5880\rho^{27} + 7200\rho^{29})\cos^2\eta$$

$$+ (12\rho^2 - 80\rho^4 + 280\rho^6 - 720\rho^8 + 1540\rho^{10} - 2912\rho^{12} + 5040\rho^{14} - 8160\rho^{16} + 12540\rho^{18}$$

$$- 18480\rho^{20} + 26312\rho^{22} - 36400\rho^{24} + 49140\rho^{26} - 64960\rho^{28})\cos^3\eta$$

$$+ (32\rho^3 - 240\rho^5 + 960\rho^7 - 2800\rho^9 + 6720\rho^{11} - 14112\rho^{13} + 26880\rho^{15} - 47520\rho^{17} + 79200\rho^{19}$$

$$- 125840\rho^{21} + 192192\rho^{23} - 283920\rho^{25} + 407680\rho^{27})\cos^4\eta$$

$$+ (80\rho^4 - 672\rho^6 + 3024\rho^8 - 9856\rho^{10} + 26208\rho^{12} - 60480\rho^{14} + 125664\rho^{16} - 240768\rho^{18}$$

$$+ 432432\rho^{20} - 736736\rho^{22} + 1201200\rho^{24} - 1886976\rho^{26})\cos^5\eta$$

$$+ (192\rho^5 - 1792\rho^7 + 8960\rho^9 - 32256\rho^{11} + 94080\rho^{13} - 236544\rho^{15} + 532224\rho^{17}$$

$$- 1098240\rho^{19} + 2114112\rho^{21} - 3843840\rho^{23} + 6662656\rho^{25})\cos^6\eta$$

$$+ (448\rho^6 - 4608\rho^8 + 25344\rho^{10} - 99840\rho^{12} + 316800\rho^{14} - 861696\rho^{16} + 2086656\rho^{18} - 4612608\rho^{20}$$

$$+ 9472320\rho^{22} - 18304000\rho^{24})\cos^7\eta$$

$$+ (1024\rho^7 - 11520\rho^9 + 69120\rho^{11} - 295680\rho^{13} + 1013760\rho^{15} - 2965248\rho^{17} + 7687680\rho^{19}$$

$$- 18120960\rho^{21} + 39536640\rho^{23})\cos^8\eta$$

$$+ (2304\rho^8 - 28160\rho^{10} + 183040\rho^{12} - 844800\rho^{14} + 3111680\rho^{16} - 9737728\rho^{18} + 26906880\rho^{20}$$

$$- 67358720\rho^{22})\cos^9\eta$$

$$+ (5120\rho^9 - 67584\rho^{11} + 473088\rho^{13} - 2342912\rho^{15} + 9225216\rho^{17} - 30750720\rho^{19}$$

$$+ 90202112\rho^{21})\cos^{10}\eta$$

$$+ (11264\rho^{10} - 159744\rho^{12} + 1198080\rho^{14} - 6336512\rho^{16} + 26557440\rho^{18} - 93929472\rho^{20})\cos^{11}\eta$$

$$+ (24576\rho^{11} - 372736\rho^{13} + 2981888\rho^{15} - 16773120\rho^{17} + 74547200\rho^{19})\cos^{12}\eta$$

$$+ (53248\rho^{12} - 860160\rho^{14} + 7311360\rho^{16} - 43581440\rho^{18}) \cos^{13}\eta$$

$$+ (114688\rho^{13} - 1966080\rho^{15} + 17694720\rho^{17}) \cos^{14}\eta$$

$$+ (245760\rho^{14} - 4456448\rho^{16}) \cos^{15}\eta$$

$$+ (524288\rho^{15}) \cos^{16}\eta \qquad (19)$$

after terminating the expansion at the q^{15} term (inclusive). The approximation given above holds only for $\eta \leqslant \text{Arc cos } \rho$; elsewhere $B' = 0$.

The b_ℓ can be found from the inner product (e.g., Hobson, 1955, p. 42):

$$b_\ell = \left(\frac{2\ell+1}{2}\right)\!\!\int_0^\pi B\, P_\ell(\cos\eta)\, \sin\eta\, d\eta \ .$$

Hence,

$$b'_\ell = \left(\frac{2\ell+1}{2}\right)\int_\rho^1 B' P_\ell(\cos\eta)\, d(\cos\eta) \qquad (20)$$

where b_ℓ' is the approximation to b_ℓ. The lower limit of this last integral reflects the fact that $B' = 0$ in the region invisible to the satellite. The b_ℓ' will be used in place of b_ℓ in what follows.

It is easier to compute the b_ℓ' numerically than to give analytical expressions for them. Using the basic equation

$$r = \frac{a(1 - e^2)}{1 + e\cos f} \qquad (21)$$

and the numerical values for R_A, a, and e for Lageos result in

$$\rho = 0.520049\,(1 + e\cos f)$$

so that

$$\rho^n \cong (0.520049)^n (1 + ne\cos f)$$

since e is small. This equation, together with (19) and (20), yield the b_ℓ' listed in Table V for ℓ running from 0 to 6. The values for b_ℓ' in turn allow

$$B' \cong \sum_{\ell=0}^{6} b'_\ell\, P_\ell(\cos\eta)$$

to be computed. This function is shown in Figure 5 plotted against η together with the exact analytical expression for B. Both curves assume Lageos to be in a circular orbit. The figure shows that the approximation for B is not as good as the one for D.

34

4. Earth Albedo

Now that the formalism for the albedo acceleration has been developed, it is time to consider what model to use for the earth's albedo for short wavelengths. Since only the zonal terms in the albedo are retained ($K = 0$), it comes down to the matter of choosing $\bar{A}_{001}$, $\bar{A}_{101}$, $\bar{A}_{201}$, etc. Stephens et al. (1981) summarized several years' worth of satellite data from which a set of coefficients can be derived. They give the monthly zonal mean albedos for latitude bands 10 degrees wide, plus the yearly average for each band (see their Table 4b). Assuming that the albedo values refer to the midpoint of each band (so that the value for $60°N - 70°N$ is taken to be at $65°N$, for example), one can do a least-squares fit to the data with a sum of Legendre polynomials.

The resulting coefficients $\bar{A}_{001}$ through $\bar{A}_{401}$ for each month, which come from fitting the first five polynomials, are shown in Figure 6. This figure shows that the coefficients for even N are all fairly constant throughout the year. The coefficients for odd N show a distinct sinusoidal behavior with a period of one year. However, $\bar{A}_{301}$ is not sinusoidal about zero like $\bar{A}_{101}$. Rather, it shows a constant offset which is presumably due to the presence of the large Antarctic ice cap. The coefficient $\bar{A}_{001}$ gives a rough measure of how good the fit is, since its time-averaged value is actually 0.30, varying only between 0.29 and 0.32 during the year (Stephens et al., 1981, p. 9744). The least-squares estimate is consistently high, but only a little.

Clearly it will do no great violence to the data to take

$$
\begin{aligned}
A(\theta, \lambda) = 0.30 & \quad \bar{P}_{0,0}(\cos\theta) \\
+ [0.05 \cos f_S] & \quad \bar{P}_{1,0}(\cos\theta) \\
+ 0.10 & \quad \bar{P}_{2,0}(\cos\theta) \\
+ [-0.01 + 0.03 \cos f_S] & \quad \bar{P}_{3,0}(\cos\theta) \\
+ 0.04 & \quad \bar{P}_{4,0}(\cos\theta)
\end{aligned}
\tag{22}
$$

as the model for the earth's albedo. This is a hybrid expression: $\bar{A}_{001}$ is Stephens et al.'s (1981) time-averaged value, while the other coefficients are based on Figure 6. Obviously a more accurate expression could be obtained by analyzing Stephens et al.'s (1981) original data, but (22) is good enough for the purposes considered here (see Figures 6 and 7).

Note that the coefficients for even N are assumed to be constant. The time-varying parts of $\bar{A}_{101}$ and $\bar{A}_{301}$ are modeled with $\cos f_S$; this can be done due to the fortuitous circumstance of perihelion passage occurring near the first of the year. Note also that the albedo is dominated by the zeroth and second degree harmonics.

35

5. Lageos

The analytical formalism and the albedo model will now be applied to the Lageos satellite. Lageos has the following parameters in addition to those shown in Table I:

$$\Omega \cong \Omega_0 + \dot{\Omega}\,(t - t_0)$$
$$\omega \cong \omega_0 + \dot{\omega}\,(t - t_0)$$

where

$$\Omega_0 = +28.5596 \text{ deg}$$
$$\omega_0 = +171.9271 \text{ deg}$$
$$t_0 = 2902.5 \text{ days} \qquad \text{(Julian Date)}.$$

For further information about Lageos, see Smith and Dunn (1980) and Rubincam (1982).

The Lageos values will be used to compute R, S, and W via (17), (18) and the modification of R which yields S. Other values necessary for the computation are those given in Table II, the d_L given in Table IV, the $b_\ell{}'$ given in Table V, and the $\overline{A}_{N01}$ given by (22). Also, the earth's orbit about the sun will be taken to be circular, so that $(a_S/r_S) = 1$. Further,

$$\omega_S + f_S = (\omega_S + f_S)_0 + (\dot{\omega} + \dot{f})\,(t - t_0)$$

where

$$(\omega_S + f_S)_0 = 42.0087 \text{ deg}.$$

The subscripts will run between the following values in the summations: $0 \leqslant N \leqslant 4$, $0 \leqslant L \leqslant 4$, and $0 \leqslant \ell \leqslant 5$.

What does one get for R, S, and W using all of this data? The answer is: thousands of terms for each of the accelerations, for each value of N. Many of the terms are zero, since $1 - (-1)^{N+L+\ell}$ and the 3-j symbols are often zero. A computer program is necessary to make all of the calculations. It also proves convenient to gather together all of the terms with the same frequency with the aid of the computer.

Sample calculations for R, S, and W as they vary over one revolution are shown in Figures 8 – 12 for the major terms in the albedo N = 0 and N = 2. In all of these figures the sun is on the equator and Lageos passes directly over the subsolar point. The correct qualitative behavior for R when N = 0 (Levin, 1962; see also Anselmo et al., 1983) is evident in Figure 8. Here the acceleration is

roughly zero in the shadow, rises to a maximum when Lageos is directly over the subsolar point (where the reflection is strongest), and then falls off symmetrically towards zero. Likewise Figure 10 shows the correct qualitative antisymmetric behavior for S (Levin, 1962; Anselmo et al., 1983): nearly zero in the shadow, and then negative as the satellite approaches the subsolar point and the sunny area pushes Lageos against the direction of motion. S is zero because of symmetry when Lageos is over the subsolar point; then positive as the sunny area pushes Lageos along its way. Note that the maximum amplitude for S is about an order-of-magnitude less than that for R, also in agreement with Levin (1962).

One way in which Figure 8 differs from Levin's figure is that his R has a flat top. Also, the humps in Levin's S are separated by a stretch where S is zero, while the humps of Figure 10 are joined together. These differences are due to Levin's oversimplification of the problem.

No figure shows W for N = 0; it is zero over the entire orbit, by symmetry. However, W for N = 2 is shown in Figure 12.

The long-period perturbations in the Keplerian elements a, e, ω, I and Ω for N = 0 are found next using the Gaussian form of Lagrange's planetary equations. Perturbations in the mean anomaly M are not considered. The assumption of a circular orbit will be dropped when considering changes in a, e, and ω but retained when considering changes in I and Ω.

The change in the semimajor axis with time is given by (e.g., Blanco and McCuskey, 1961, p. 178)

$$\frac{da}{dt} = \frac{2}{nr\sqrt{1-e^2}} [(er \sin f)R + a(1 - e^2)S]$$

$$= \frac{2}{n\sqrt{1-e^2}} [(e \sin f)R + (1 + e \cos f)S]$$

where n is the mean motion and use has been made of (21).

Substituting R_0' for R and

$$S' \cong S_0' + (e \cos f) S_1' \tag{23}$$

in the above equation yields

$$\frac{da}{dt}\bigg|_{l.p.} \cong \frac{2e}{n\sqrt{1-e^2}} [(\sin f)R_0' + \cos f (S_0' + S_1')] \tag{24}$$

37

to first order in e for the long-period (l.p.) part of da/dt. The prime denotes the parts of R and S which contribute to the long-period perturbations, while R_o' and S_o' are the portions of R' and S' respectively which are independent of the eccentricity. S' is written to first order in e; hence the term $(e \cos f) S_1'$ in (23). The factor $e \cos f$ ultimately comes from the eccentric part of ρ. A term $2 S_o'/(n\sqrt{1-e^2})$ which appears after making the substitution of (23) into (24) has been dropped, since it contributes only short-period terms.

The long-period terms in R and S are all of those which contain $\pm(\omega+f)$ inside the trigonometric argument; all other terms are short-period. According to the computer program they are

$$
R_o' = 10^{-12} \left\{
\begin{array}{l}
+ 11.729 \cos[(\omega_S + f_S) - (\omega+f) \quad] \\
- 11.729 \cos[(\omega_S + f_S) + (\omega+f) \quad] \\
+ 19.829 \cos[(\omega_S + f_S) - (\omega+f) - \Omega] \\
+ 40.293 \cos[(\omega_S + f_S) + (\omega+f) - \Omega] \\
+ 1.735 \cos[(\omega_S + f_S) - (\omega+f) + \Omega] \\
+ 0.854 \cos[(\omega_S + f_S) + (\omega+f) + \Omega]
\end{array}
\right\} \quad ms^{-2} \tag{25}
$$

$$
S_o' = 10^{-12} \left\{
\begin{array}{l}
- 1.215 \sin[(\omega_S + f_S) - (\omega+f) \quad] \\
- 1.215 \sin[(\omega_S + f_S) + (\omega+f) \quad] \\
- 2.054 \sin[(\omega_S + f_S) - (\omega+f) - \Omega] \\
+ 4.174 \sin[(\omega_S + f_S) + (\omega+f) - \Omega] \\
- 0.180 \sin[(\omega_S + f_S) - (\omega+f) + \Omega] \\
+ 0.088 \sin[(\omega_S + f_S) + (\omega+f) + \Omega]
\end{array}
\right\} \quad ms^{-2} \tag{26}
$$

$$
S_1' = 10^{-12} \left\{
\begin{array}{l}
+ 0.754 \sin[(\omega_S + f_S) - (\omega+f) \quad] \\
+ 0.754 \sin[(\omega_S + f_S) + (\omega+f) \quad] \\
+ 1.275 \sin[(\omega_S + f_S) - (\omega+f) - \Omega] \\
- 2.591 \sin[(\omega_S + f_S) + (\omega+f) - \Omega] \\
+ 0.112 \sin[(\omega_S + f_S) - (\omega+f) + \Omega] \\
- 0.055 \sin[(\omega_S + f_S) + (\omega+f) + \Omega]
\end{array}
\right\} \quad ms^{-2} \tag{27}
$$

Substituting (25) – (27) in (24) and using (16) yields for the change in semimajor axis

$$
\Delta a - \Delta a_o = \left.
\begin{array}{l}
- 0.40 \cos[(\omega_S + f_S) - \omega \quad] \\
- 0.62 \cos[(\omega_S + f_S) + \omega \quad] \\
- 0.95 \cos[(\omega_S + f_S) - \omega - \Omega] \\
+ 3.82 \cos[(\omega_S + f_S) + \omega - \Omega] \\
- 0.05 \cos[(\omega_S + f_S) - \omega + \Omega] \\
+ 0.03 \cos[(\omega_S + f_S) + \omega + \Omega]
\end{array}
\right\} \quad mm \tag{28}
$$

after integrating and dropping some more short-period terms. Here Δa_0 is Δa at time t_0. The per-turbations in the semimajor axis are thus quite small. The largest term has an amplitude of 3.82mm and a period of 833 days. A graph of (28) is shown in Figure 13.

The change in eccentricity with time is given by (e.g. Blanco and McCuskey, 1961, p. 178)

$$\frac{de}{dt} = \frac{\sqrt{1-e^2}}{nae}\left\{(e\sin f)\,R + \left[\frac{a(1-e^2)}{r} - \frac{r}{a}\right]S\right\} \quad ,$$

so that

$$\left.\frac{de}{dt}\right|_{l.p.} \cong \frac{\sqrt{1-e^2}}{na}\left\{(\sin f)R_0' + (2\cos f)S_0'\right\}$$

after again making use of (21). Substituting (25) and (26) in this equation and integrating gives

$$\left[\frac{\Delta e - \Delta e_0}{e}\right] \cong 10^{-6}\left\{\begin{array}{ll} -0.844 & \cos[(\omega_S + f_S) - \omega] \\ -1.304 & \cos[(\omega_S + f_S) + \omega] \\ -2.000 & \cos[(\omega_S + f_S) - \omega - \Omega] \\ +8.028 & \cos[(\omega_S + f_S) + \omega - \Omega] \\ -0.097 & \cos[(\omega_S + f_S) - \omega + \Omega] \\ +0.066 & \cos[(\omega_S + f_S) + \omega + \Omega] \end{array}\right\} \quad (29)$$

Thus e changes by only about one part in 10^5. A graph of (29) is shown in Figure 13 also.

Proceeding in similar fashion,

$$\frac{d\omega}{dt} = \frac{\sqrt{1-e^2}}{-nae}\left\{(\cos f)R - \sin f\left[1 + \frac{r}{a(1-e^2)}\right]S + \left[\frac{er\sin(\omega+f)\cot I}{a(1-e^2)}\right]W\right\}$$

(e.g. Blanco and McCuskey, 1961, p. 178), so that

$$\left.\frac{d\omega}{dt}\right|_{l.p.} \cong \frac{\sqrt{1-e^2}}{nae}\left\{(\cos f)R_0' - (2\sin f)S_0'\right\}$$

39

and the term containing W has been ignored, since it is multiplied by e. Using (25) and (26) and integrating yields

$$
\begin{aligned}
\Delta\omega - \Delta\omega_o \;=\; & -0.174 \cos[(\omega_S + f_S) - \omega \quad] \\
& + 0.269 \cos[(\omega_S + f_S) + \omega \quad] \\
& - 0.412 \cos[(\omega_S + f_S) - \omega - \Omega] \\
& - 1.656 \cos[(\omega_S + f_S) + \omega - \Omega] \\
& - 0.020 \cos[(\omega_S + f_S) - \omega + \Omega] \\
& - 0.014 \cos[(\omega_S + f_S) + \omega + \Omega] \quad \text{arc sec} \;\cdot
\end{aligned}
$$

See Figure 14 for a graph.

The equations above give all of the long-period terms for the stipulated conditions on N, L, and ℓ. Unfortunately, the corresponding equations for the perturbations in the inclination and longitude of node contain a great many more terms. This is because W, which controls these perturbations, contains a large number of contributing terms, unlike R and S. Only those terms in ΔI and $\Delta\Omega$ which have an amplitude greater than 10^{-4} arc sec will be listed here:

$$
\begin{aligned}
\Delta I - \Delta I_o \cong 10^{-4} \; \big\{ \; & 1.795 \sin[\quad\quad\quad \Omega \;] \\
& -0.501 \sin[\quad\quad\quad 2\Omega \;] \\
& +0.395 \sin[2(\omega_S + f_S) - \Omega \;] \\
& +3.018 \sin[2(\omega_S + f_S) - 2\Omega \;] \\
& +0.205 \sin[2(\omega_S + f_S) - 3\Omega \;] \\
& -0.141 \sin[2(\omega_S + f_S) - 4\Omega \;] \\
& -0.191 \sin[4(\omega_S + f_S) - 4\Omega \;] \big\} \quad \text{arc sec}
\end{aligned}
$$

$$
\begin{aligned}
\Delta\Omega - \Delta\Omega_o = 10^{-4} \; \big\{ \; & 3.956 \cos[\quad\quad\quad\quad \Omega \;] \\
& +0.360 \cos[\quad\quad\quad 2\Omega \;] \\
& -0.257 \cos[2(\omega_S + f_S) \quad\quad] \\
& -0.870 \cos[2(\omega_S + f_S) - \Omega \;] \\
& +1.234 \cos[2(\omega_S + f_S) - 2\Omega \;] \\
& -0.115 \cos[2(\omega_S + f_S) - 3\Omega \;] \big\} \quad \text{arc sec}
\end{aligned}
$$

These perturbations are small.

These expressions are again derived from the classical equations (e.g.,Blanco and McCuskey, 1961, p. 178). W itself is not given. For graphs of the above perturbations, see Figures 13 and 14. There is also a secular contribution to the node:

40

$$\left. \frac{d\Omega}{dt} \right|_{\text{sec}} = -7.856 \times 10^{-4} \text{ arc sec yr}^{-1}$$

which is also small. This completes the derivation of the perturbations in the Keplerian elements for $N = 0$.

The perturbations due to the higher harmonics ($N > 0$) in the albedo (22) are generally smaller than those for $N = 0$. For instance, the largest term in R_0' for $N = 2$ yields an amplitude of 0.29mm for the perturbation in the semimajor axis. Since the perturbations for $N = 0$ are already small, the perturbations for $N > 0$ will not be computed, with one exception. It turns out that the $N = 2$ and $N = 4$ harmonics contribute significantly to the secular motion of the node, being $+8.390 \times 10^{-4}$ and $+2.310 \times 10^{-4}$ arc sec yr^{-1}, respectively. The second degree term more than cancels the zeroth degree term, giving a total of

$$\left. \frac{d\Omega}{dt} \right|_{\text{sec}} \cong +2.844 \times 10^{-4} \text{ arc sec yr}^{-1}$$

for all three terms.

6. Discussion

The formalism developed here results in some rather lengthy equations for the albedo accelerations. However, a virtue of these equations is that they hold whether the satellite sees the terminator or not; in other words, they are perfectly valid for any sun-satellite geometry. Hence there is no need for separate equations for the terminator-visible and the terminator-invisible cases, as in past treatments.

Application of the formalism to Lageos' orbit shows the effect of sunlight diffusely reflected from a uniform earth to be quite small. The periodic perturbations in the node Ω, for instance, are far below the residuals level of about 0.03 arc sec of the satellite laser ranging data (Rubincam, 1984, Figure 2). Also, the semimajor axis a is perturbed at the 5mm level over a period of 833 days. This is smaller than the effect of some individual solar eclipses on the orbit of Lageos. The eclipse of 28 March 1979, for example, increased the semimajor axis by about 17.6mm within the space of an hour (Rubincam and Weiss, 1985). The albedo perturbations in e, I, and ω are likewise tiny. (Interestingly, the perturbations in a, e, and ω are dominated by the radial acceleration R.) The perturbations due to the higher harmonics ($N > 0$) in the albedo are also small. Hence diffuse reflection plays only a minor role in long-period perturbations in Lageos' orbit.

41

It is clear from the periodic nature of (28) that Lambertian reflection cannot explain the observed secular decay of 1.1mm day^{-1} in the semimajor axis (e.g., Rubincam, 1982). This has been attributed to charged particle drag (Afonso et al., 1980; Mignard, 1981; Rubincam, 1982; Afonso et al., 1985). Morgan (1984), however, suggests the decay may be caused by forward scattering due to a morning-evening asymmetry in the albedo.

Lambertian reflection cannot explain the observed unmodeled along-track variations in acceleration, either. These long-period variations have magnitude $\sim 2 \times 10^{-12}$ ms^{-2} (e.g., Rubincam, 1985; Anselmo et al., 1983). It is obvious from (27) that the along-track albedo acceleration is of magnitude $e \times 2.5 \times 10^{-12}$ ms^{-2} = 0.01×10^{12} ms^{-2}. This is two orders of magnitude too small to explain the observations.

The physical reason why the long-period variations in S depend on the eccentricity e is as follows. Consider the effect of a single surface element on a circular orbit. The surface element reflects according to Lambert's law. On the arc where the satellite approaches the element radiation pressure pushes the satellite against the direction of motion, giving a negative contribution to S. Correspondingly on the arc where the satellite moves away from the element the satellite is pushed in the direction of motion, giving a positive contribution to S. The positive and negative contributions will exactly cancel when summed over a circular orbit because of the symmetry of the diffuse reflection required by Lambert's law. The same will obviously hold true for a sum over surface elements. Hence there can be no long-period variations in along-track acceleration for a circular orbit; only short-period. An eccentric orbit must be invoked to give the asymmetry needed to produce long-period variations in S; thus the appearance of e.

This argument will hold regardless of the changes in albedo across the face of the earth. Therefore a north-south asymmetry in the albedo cannot be invoked to explain the observed variations in along-track acceleration as by Anselmo et al. (1983), at least not with Lambertian reflection. Walch (1982) also finds Lambert's law inadequate to explain the observations. He numerically modeled a combination of Lambertian reflection, specular reflection, and infrared radiation using a zonal albedo. His resulting acceleration is about an order-of-magnitude smaller than observed. This is still an order-of-magnitude larger than that computed here. The difference is presumably due to his inclusion of specular reflection, which is not considered here.

What then is causing the observed variations in along-track acceleration? One possibility is fluctuations in charged particle drag (Afonso et al., 1985; Rubincam, 1982). Another is variations in forward scattering (Morgan, 1984).

How well do the assumptions made here mimic reality? There have been some obvious simplifications: higher harmonics and tesseral harmonics in the albedo, a wavelength-dependent albedo,

an oblate earth, a ragged terminator, etc. have all been neglected. Perhaps more serious is the assumption of a time-averaged albedo, rather than a time-varying albedo. Also, more Legendre polynomials could certainly be used to improve the approximation for B, i.e., bring the dashed line closer to the solid line in Figure 5.

All of the above probably produced negligible error compared to the main assumption: that the earth reflects sunlight according to Lambert's law. In fact the ways in which the earth reflects light are still poorly understood (Stephens et al., 1981, p. 9741). Clouds and land behave somewhat like Lambert's law (Jacobowitz, 1981; Stowe and Taylor, 1981; Gube, 1982, pp. 57-58), but the oceans display a distinct anisotropic reflectance pattern with a strong specular component (Stowe and Taylor, 1981). Snow and ice are also non-Lambertian reflectors (Stephens et al. 1981, p. 9741). Hence the main future endeavor in this field should be in pursuing laws of reflectance more realistic than Lambert's law. However, the problem will become much more complicated because of angular dependence as well as the space and time variations of reflecting surfaces. A start has been made in this direction with specular reflection (Walch, 1982) and forward scattering (Morgan, 1984).

As for the present formalism, it can be modified to examine the perturbations in Lageos' orbit due to infrared radiation. These can then be compared to Sehnal's (1981) results. This work is now in progress.

Acknowledgments

APPENDIX 1

This appendix shows that the force in Lambert's law cannot be written as the gradient of a potential .

Suppose the satellite's position is at $\vec{r}_1$ in Figure 3; the force is directed along $\vec{r}_1$ and is proportional to

$$\frac{\vec{r}_1 \cos \beta}{r_1^3} = \left(\frac{x_1 \hat{x}_1 + y_1 \hat{y}_1 + z_1 \hat{z}_1}{r_1^3}\right)\left(\frac{z_1}{r_1}\right)$$

$$= \left(\frac{x_1 z_1}{r_1^4}\right) \hat{x}_1 + \left(\frac{y_1 z_1}{r_1^4}\right) \hat{y}_1 + \left(\frac{z_1^2}{r_1^4}\right) \hat{z}$$

where $r_1^2 = x_1^2 + y_1^2 + z_1^2$. If this force were derivable from a potential, then one could write $\vec{r}_1 = \nabla V$ where $(\partial V/\partial x) = x_1 z_1/(x_1^2 + y_1^2 + z_1^2)^2$, etc. apart from constant multiplicative factors. Then it should certainly be true that

$$\frac{\partial \left(\dfrac{\partial V}{\partial y_1}\right)}{\partial z_1} = \frac{\partial \left(\dfrac{\partial V}{\partial z_1}\right)}{\partial y_1}$$

Working this out implies that

$$\frac{y_1}{(x_1^2 + y_1^2 + z_1^2)^2} = 0.$$

Since y_1 is not necessarily equal to zero, the above equation cannot always hold. Hence there can be no Lambert law potential.

It is easy to see physically why this is so: the work done over a closed circuit is not zero. Consider taking a particle around the elementary circuit ABCD in Figure 3. The circuit is assumed for simplicity to lie in the $y_1 - z_1$ plane. No work is done over circular arcs BC and DA since the force is perpendicular to the path. Over AB the work done is $\Delta r_1 \cos \beta_1 / r_1^2$, apart from constant factors where β_1 is the angle between AB and the z_1 axis. Likewise the work done over CD is $-\Delta r_1 \cos \beta_2 / r_1^2$, where β_2 is the angle between CD and the z_1 axis. The net work is thus $\Delta r_1 (\cos \beta_1 - \cos \beta_2)/r_1^2$. This is not zero, since $\beta_1 \neq \beta_2$. Hence the force is not conservative and therefore not derivable from a potential.

44

APPENDIX 2

The quantum-mechanical spherical harmonics $Y_L{}^J(\theta,\lambda)$ are related to the geophysical spherical harmonics $Y_{LJj}(\theta,\lambda)$ by the equation

$$Y_L{}^J(\theta,\lambda) = \frac{(-1)^{\frac{J+|J|}{2}}}{[4\pi(2-\delta_{oJ})]^{1/2}}\left[\bar{Y}_{L|J|1}(\theta,\lambda) - (1-2\delta_{J|J|})\,i\,\bar{Y}_{L|J|2}(\theta,\lambda)\right]$$

The inverse relations are

$$\bar{Y}_{LJ1}(\theta,\lambda) = [\pi(2-\delta_{oJ})]^{1/2}[(-1)^J Y_L{}^J(\theta\,\lambda) + Y_L{}^{-J}(\theta\,\lambda)]\,, \qquad J \geq 0$$

$$\bar{Y}_{LJ2}(\theta,\lambda) = \frac{[\pi(2-\delta_{oJ})]^{1/2}}{i}[(-1)^J Y_L{}^J(\theta,\lambda) - Y_L{}^{-J}(\theta,\lambda)]\,, \qquad J \geq 0$$

The geophysical spherical harmonics are defined by

$$\bar{Y}_{LJ1}(\theta,\lambda) = \bar{P}_{L,J}(\cos\theta)\,\cos\,m\lambda$$

$$\bar{Y}_{LJ2}(\theta,\lambda) = \bar{P}_{L,J}(\cos\theta)\,\sin\,m\lambda$$

where

$$\bar{P}_{L,J}(\cos\theta) = \left[(2-\delta_{oJ})(2L+1)\frac{(L-J)!}{(L+J)!}\right]^{1/2}P_{L,J}(\cos\theta)$$

so that

$$\int_0^{2\pi}\int_0^{\pi}\bar{Y}_{LJj}(\theta\,\lambda)\,\bar{Y}_{L'J'j'}(\theta\lambda)\,\sin\theta\,d\theta\,d\lambda = 4\pi\,\delta_{LL'}\,\delta_{JJ'}\,\delta_{jj'}.$$

In other words, the geophysical spherical harmonics follow Kaula's (1966, p. 7) 4π normalization. Note that $\bar{Y}_{L02}(\theta,\lambda) = 0$. Likewise any coefficient $C_L{}^J$ of $Y_L{}^J(\theta,\lambda)$ is related to the coefficients $\bar{C}_{L|J|1}$, $C_{L|J|2}$ of the respective $\bar{Y}_{L|J|1}(\theta,\lambda)$, $\bar{Y}_{L|J|2}(\theta,\lambda)$ by

$$C_L{}^J = [\pi(2 - \delta_{oJ})]^{1/2} (-1)^{\frac{J+|J|}{2}} \; [\overline{C}_{L|J|1} + (1 - 2\delta_{J|J|}) i \, \overline{C}_{L|J|2}]$$

and

$$\overline{C}_{LJ1} = \frac{1}{[4\pi(2 - \delta_{oJ})]^{1/2}} \left[(-1)^J C_L{}^J + C_L{}^{-J} \right] , \qquad\qquad J \geqslant 0$$

$$\overline{C}_{LJ2} = \frac{i}{[4\pi(2 - \delta_{oJ})]^{1/2}} \left[(-1)^J C_L{}^J - C_L{}^{-J} \right] , \qquad\qquad J \geqslant 0$$

Obviously, $\overline{C}_{L02} = 0$.

References

Afonso, G., Barlier, F., Berger, C., and Mignard, F.· 1980, 'Effet du freinage atmospherique et de la trainee electrique sur la trajectoire du satellite·Lageos,' *C. R. Acad. Sci.Paris*, 290B, 445-448.

Afónso, G., Barlier, F., Berger, C., Mignard, F., and Walch, J.J.: 1985, 'Reassessment of the Charge and Neutral Drag of Lageos and Its Geophysical Implications,' *J. Geophys. Res.*, in press.

Alonso, M. and Finn, E.J.: 1968, *Fundamental University Physics*, Vol. III, Addison-Wesley, Reading, Mass., U.S.A.

Anselmo, L., Farinella, P., Milani, A., and Nobili, A.M.: 1983, 'Effects of the Earth-reflected Sunlight on the Orbit of the LAGEOS Satellite,' *Astron. Astrophys.*, 117, 3-8.

Bess, T.D., and Smith, G.L.: 1981, 'Time and Space Spectra of Earth-Emitted Radiation at Large Scales,' in *Fourth Conference on Atmospheric Radiation*, American Meteorological Society, Boston, pp. 128-131.

Blanco, V.M., and McCuskey, S.W.: 1961, *Basic Physics of the Solar System*, Addison-Wesley, Reading, Mass., U.S.A.

Brown, E.B.: 1965, *Modern Optics*, Reinhold, New York.

Caputo, M.: 1967, *The Gravity Field of the Earth*, Academic Press, New York.

Gube, M.: 1982,'Planetary Albedo Estimtes from Meteosat Data,' *ESA J.*, 6, 53-69.

Hickey, J.R., Stowe, L.L., Jacobowitz, H., Pelligrino, P., Maschhoff, R.H., House, F., and Vonder Haar, T.H.: 1980, 'Initial Solar Irradiance Determinations from Nimbus 7 Cavity Radiometer Measurements,' *Science, 208*, 281-283.

Hobson, E.W.: 1955, *The Theory of Spherical and Ellipsoidal Harmonics*, Chelsea, New York.

Jacobowitz, H.: 1981, 'The Effect of Angular Distribution Models on the Estimation of the Earth's Albedo,' in *Fourth Conference on Atmospheric Radiation*, American Meteorological Society, Boston, pp. 146-148.

Kaula, W.M.: 1966, *Theory of Satellite Geodesy*, Blaisdell, Waltham, Mass., U.S.A.

Lautman, D.A.: 1977a, 'Perturbations of a Close-Earth Satellite Due to Sunlight Diffusely Reflected from the Earth. I: Uniform Albedo,' *Celest. Mech., 15*, 387-420.

Lautman, D.A.: 1977b, 'Perturbations of a Close-Earth Satellite Due to Sunlight Diffusely Reflected from the Earth. II: Variable Albedo,' *Celest. Mech., 16*, 3-25.

Levin, E.: 1962, 'Reflected Radiation Received by an Earth Satellite,' *ARS J., 32*, 1328-1331.

Lochry, R.R.: 1966, 'The Perturbative Effects of Diffuse Radiations from the Earth and Moon on Close Satellites,' Ph.D. thesis, University of California at Los Angeles, 177 pp.

Longman, I.M.: 1962, 'A Green's Function for Determining the Deformation of the Earth Under Surface Mass Loads, 1: Theory,' *J. Geophys. Res.,* 845-850.

Mignard, F.: 1981, 'Action de l'atmosphere neutre et ionisee sur le mouvement d'un satellite-Application a Lageos, '*Ann. Geophys., 37*, 247-252.

Merzbacher, E.: 1970, *Quantum Mechanics,* Second Edition, Wiley, New York.

Morgan, W.J.: 1984, 'Morning/Evening Difference in Earth's Albedo and the Deceleration of Lageos, (Abstract), *EOS, 65*, 855.

Prior, E.M.: 1970, 'Earth Albedo Effects on the Orbital Variations of Echo I and PAGEOS I,' in B. Morando (ed.), *Dynamics of Satellites 1969,* Springer-Verlag, Berlin, pp. 303-312.

Rotenberg, M., Bivins, R., Metropolis, N., and Wooten, J.K.: 1959, *The 3-j and 6-j Symbols,* Technology Press, Cambridge, Mass., U.S.A.

Rubincam, D.P.: 1982, 'On the Secular Decrease in the Semimajor Axis of Lageos's Orbit,' *Celest. Mech., 26*, 361-382.

Rubincam, D.P.: 1984, 'Postglacial Rebound Observed by Lageos and the Effect Viscosity of the Lower Mantle,' *J. Geophys. Res., 89*, 1077-1087.

Rubincam, D.P., and Weiss, N.R.: 1985, 'The Orbit of Lageos and Solar Eclipses,' *J. Geophys. Res.*, in press.

Sehnal, L.: 1981, 'Effects of the Terrestrial Infrared Radiation Pressure on the Motion of an Artificial Satellite,' *Celest. Mech., 25*, 169-179.

Selby, S.M. (ed.): 1974, *CRC Standard Mathematical Tables*, Twenty-second Edition, CRC Press, Cleveland, Ohio, U.S.A.

Smith, D.E.: 1970, 'Earth-reflected Radiation Pressure,' in B. Morando (ed.), *Dynamics of Satellites 1969*, Springer-Verlag, Berlin, 284-294.

Smith, D.E.: 1983, 'Acceleration on Lageos Spacecraft,' *Nature, 304*, 15.

Smith, D.E., and Dunn, P.J.: 1980, 'Long Term Evolution of the Lageos Orbit,' *Geophys. Res. Letters, 7*, 437-440.

Stephens, G.L., Campbell, G.G., and Vonder Haar, T.J.: 1981, 'Earth Radiation Budgets,' *J. Geophys. Res., 86*, 9739-9760.

Stowe, L L., and Taylor, V.R.: 1981, 'Emission Characteristics of Earth and Cloud Surfaces as Measured by the ERB Scanning Channels on the Nimbus-7 Satellite,' in *Fourth Conference on Atmospheric Radiation*, American Meteorological Society, Boston, pp. 124-127.

Walch, J.J.: 1982, 'Choix d'un modele de rayonement d'albedo terrestre. Calcul pratique de son effet sur la trajectoire d'un satellite,' Third International Symposium on the Use of Artificial Satellites for Geodesy and Geodynamics, Ermioni, Greece, September.

Zerbini, S.: 1980, 'Direct Solar and Earth-albedo Radiation Pressure Effects on the Orbit of Pageos I,' *Celest. Mech., 22*, 307-334.

TABLE CAPTIONS

Table I. Notation for quantities relating to Lageos. The quantities in the first part of the table refer to Lagros' orbit, while those in the second part refer to the satellite itself. Dash (−) indicates various numerical values are assumed.

Table II. Notations for quantities relating to the sun, earth, and universe. Dash (--) indicates various numerical values are assumed. Symbols not shown in Tables I and II are defined in the text.

Table III. Unnormalized inclinations functions $F_{\ell mp}(I)$ for $\ell = 0, 1$.

Table IV. Values for d_L.

Table V. Values for b_{ℓ}' for Lageos, based on $\rho = 0.520049 \, (1 + e \cos f)$.

TABLE I

Notation for quantities relating to Lageos. The quantities in the first part of the table refer to Lageos' orbit, while those in the second part refer to the satellite itself. Dash (–) indicates various numerical values are assumed.

Quantity	Symbol	Numerical Value
Semimajor axis	a	1.227×10^7 m
Eccentricity	e	0.004
True anomaly	f	–
Inclination	I	109.9 deg
Mean motion	n	4.645×10^{-4} s^{-1}
Earth-Lageos distance	r_L	–
Argument of perigee	ω	–
Perigee rate	$\dot\omega$	– 0.2112 deg day^{-1}
Longitude of node	Ω	–
Node rate	$\dot\Omega$	0.3425 deg day^{-1}
R_A/r_L	ρ	–
Radiation coefficient	C_R	1.13
Mass	M_L	407 kg
Radius	R_L	0.3 m

TABLE II

Notation for quantities relating to the sun, earth and universe. Dash (–) indicates various numerical values are assumed. Symbols not shown in Tables I and II are defined in the text.

Quantity	Symbol	Numerical Value
Semimajor axis	a_S	1.496×10^{11} m
True anomaly	f_S	–
Inclination	I_S	23.44 deg
Earth-sun distance	r_S	–
Argument of perigee	ω_S	–
Longitude of node	Ω_S	0
Daily motion	$\dot\omega_S + \dot f_S$	0.9856 deg day^{-1}
Solar constant	F_S°	1376 W m^{-2}
Earth albedo	$A(\theta,\lambda)$	–
Radius of albedo surface	R_A	6381 km
Speed of light	c	2.998×10^8 ms^{-1}
Gravitation constant	G	6.67×10^{-11} m^3 kg^{-1}s^{-2}
Time	t	–

TABLE III

Unnormalized inclination functions $F_{\ell mp}(I)$ for $\ell = 0, 1$.

ℓ	m	p	$F_{\ell mp}(I)$
0	0	0	1
1	0	0	$(\sin I)/2$
1	0	1	$(-\sin I)/2$
1	1	0	$(1 + \cos I)/2$
1	1	1	$(1 - \cos I)/2$

TABLE IV

Values for d_L

L	d_L
0	+1/4
1	+1/2
2	+5/16
3	0
4	−3/32
5	0
6	+13/256

TABLE V

Values for b_{ℓ}' for Lageos, based on $\rho = 0.520049 \, (1 + e \cos f)$.

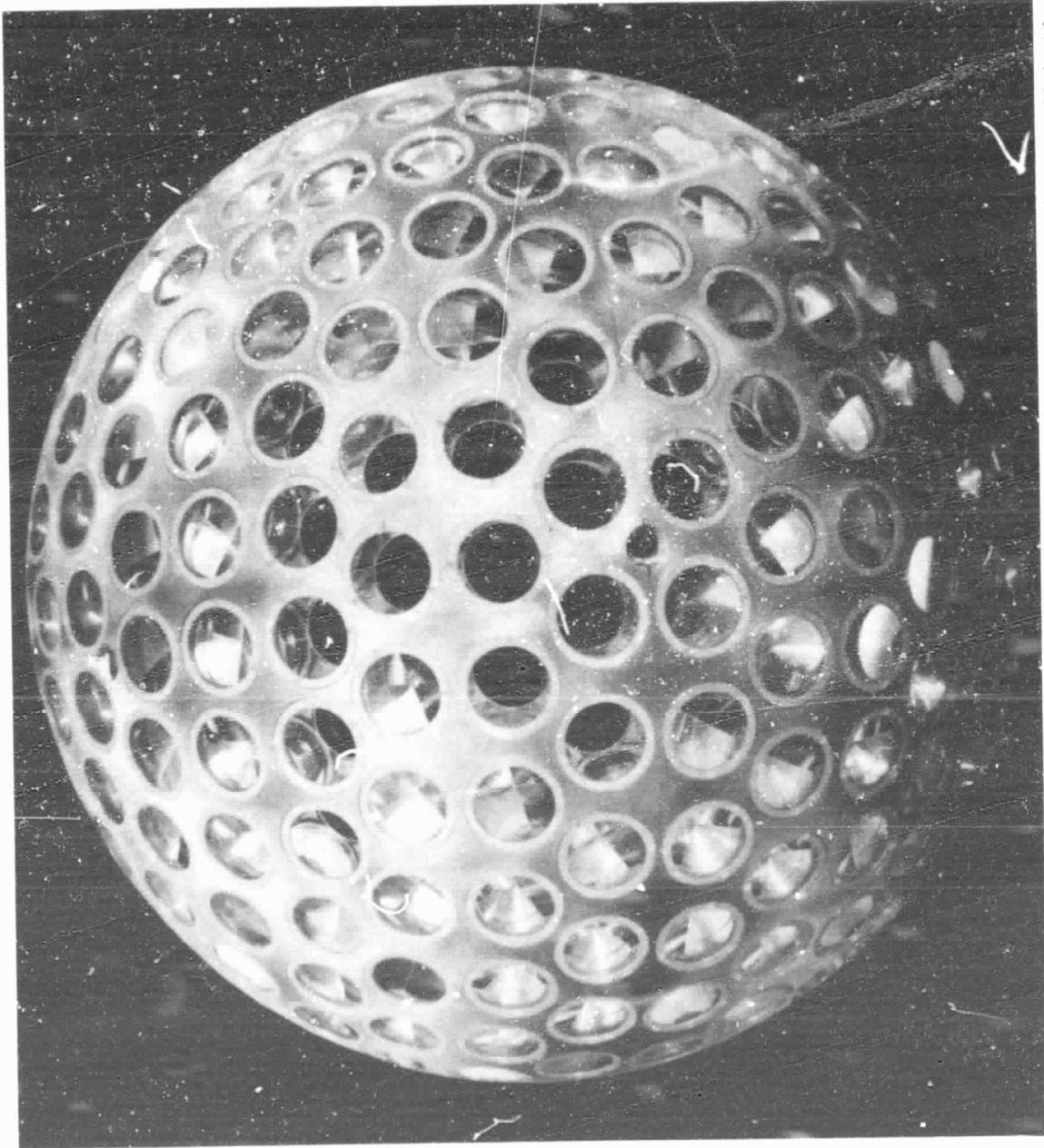| ℓ	b_{ℓ}
-1	0
0	$+0.45795 \ + \ 0.37014 \ e \cos f$
1	$+1.23068 \ + \ 1.21735 \ e \cos f$
2	$+1.64127 \ + \ 2.25323 \ e \cos f$
3	$+1.63083 \ + \ 3.20260 \ e \cos f$
4	$+1.31099 \ + \ 3.74560 \ e \cos f$
5	$+0.88601 \ + \ 2.91399 \ e \cos f$
6	$+0.50452 \ + \ 2.71441 \ e \cos f$

Figure 1. The Lageos satellite. Lageos is a completely passive satellite whose aluminum surface is studded with laser retroreflectors.
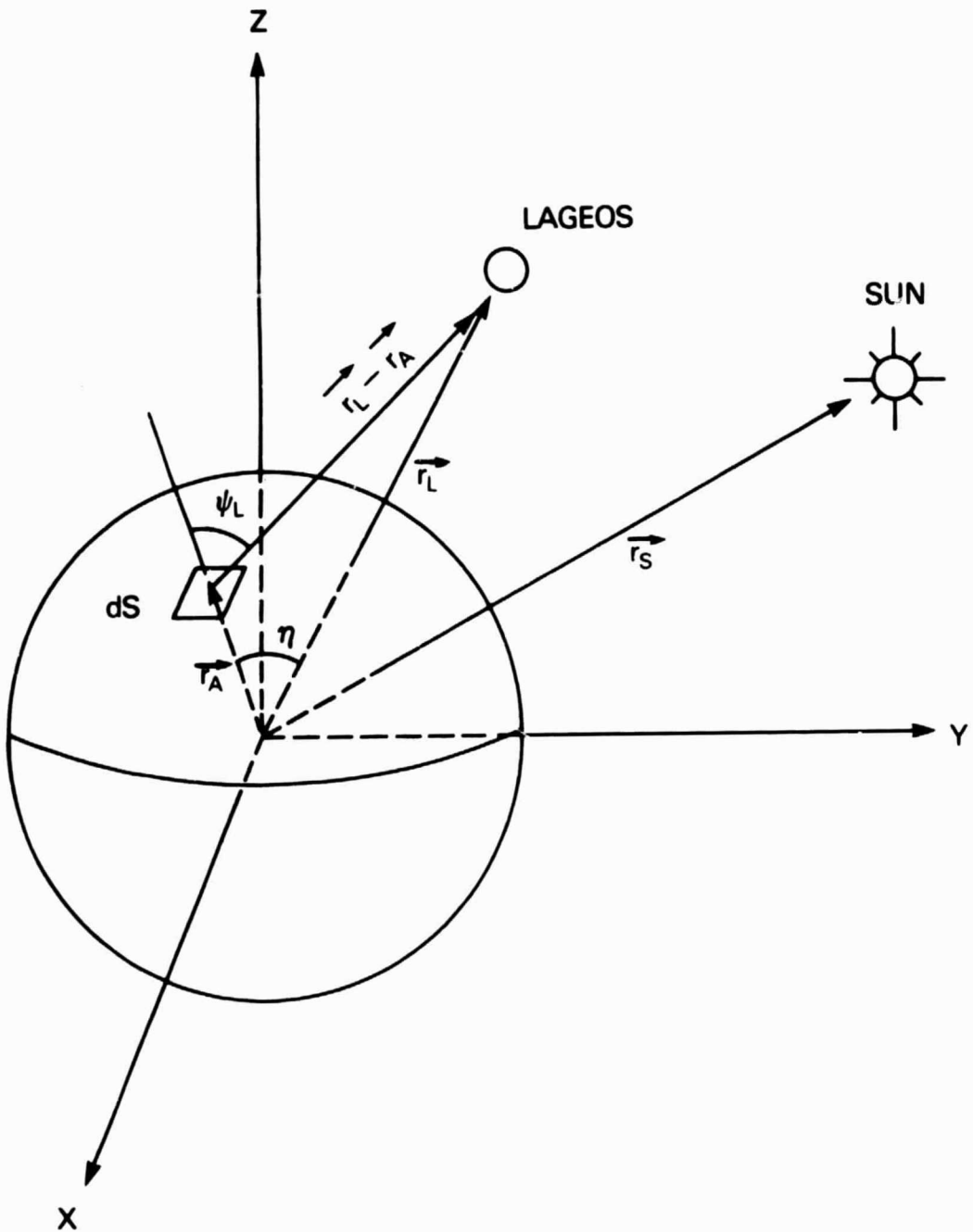
Figure 2. Positions of the sun, satellite, and surface element in the inertial coordinate system xyz. The coordinate system does not rotate around with the earth. The x-axis points to the vernal equinox and the z-axis lies along the rotation axis. Since the system is considered to be inertial, fictitious forces produced by the earth's motion around the sun are ignored.
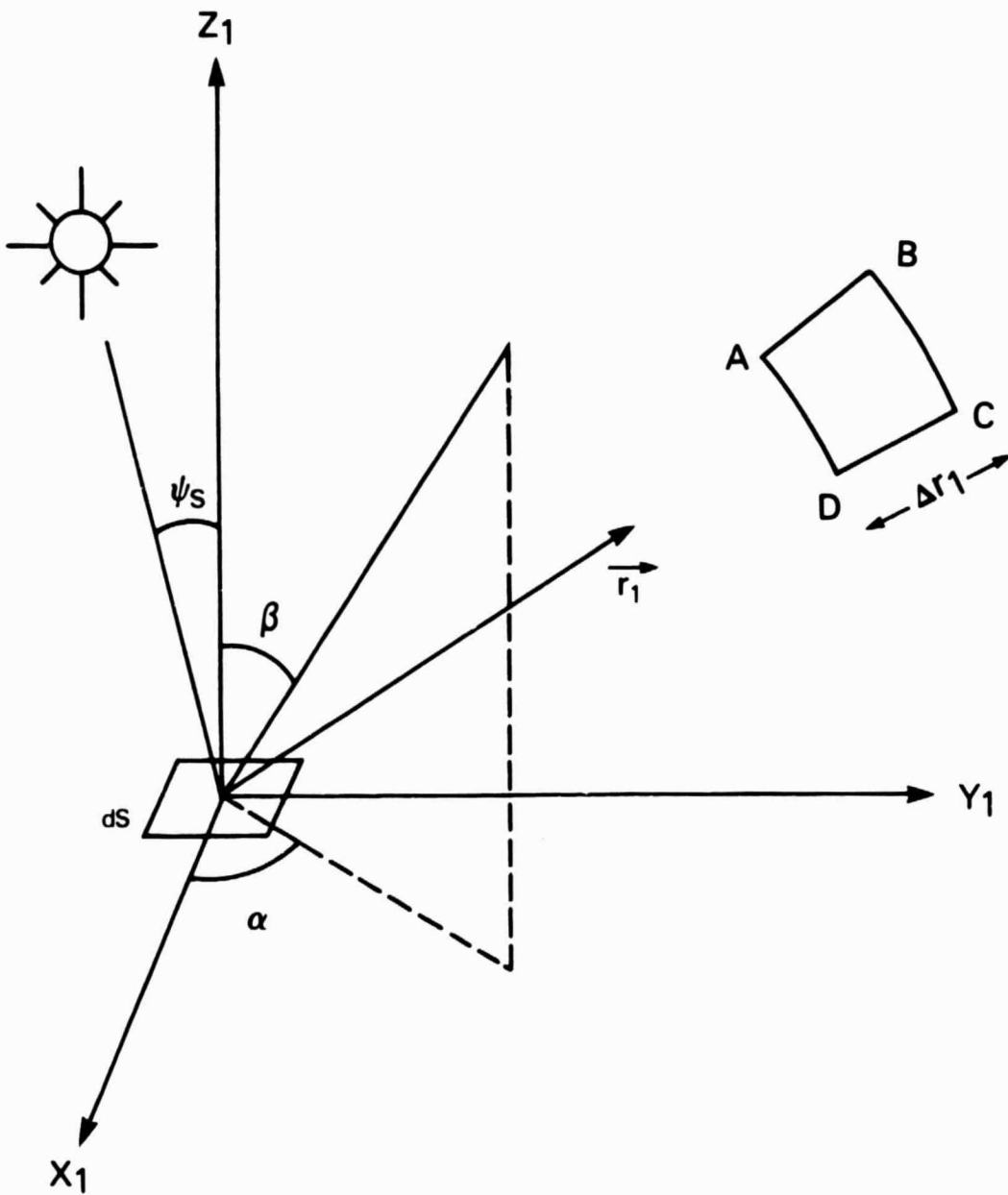
Figure 3. The local frame $x_1 y_1 z_1$ of the surface element dS. The vector $\vec{r_1}$ and the circuit ABCD are discussed in Appendix 1; otherwise they are to be ignored.
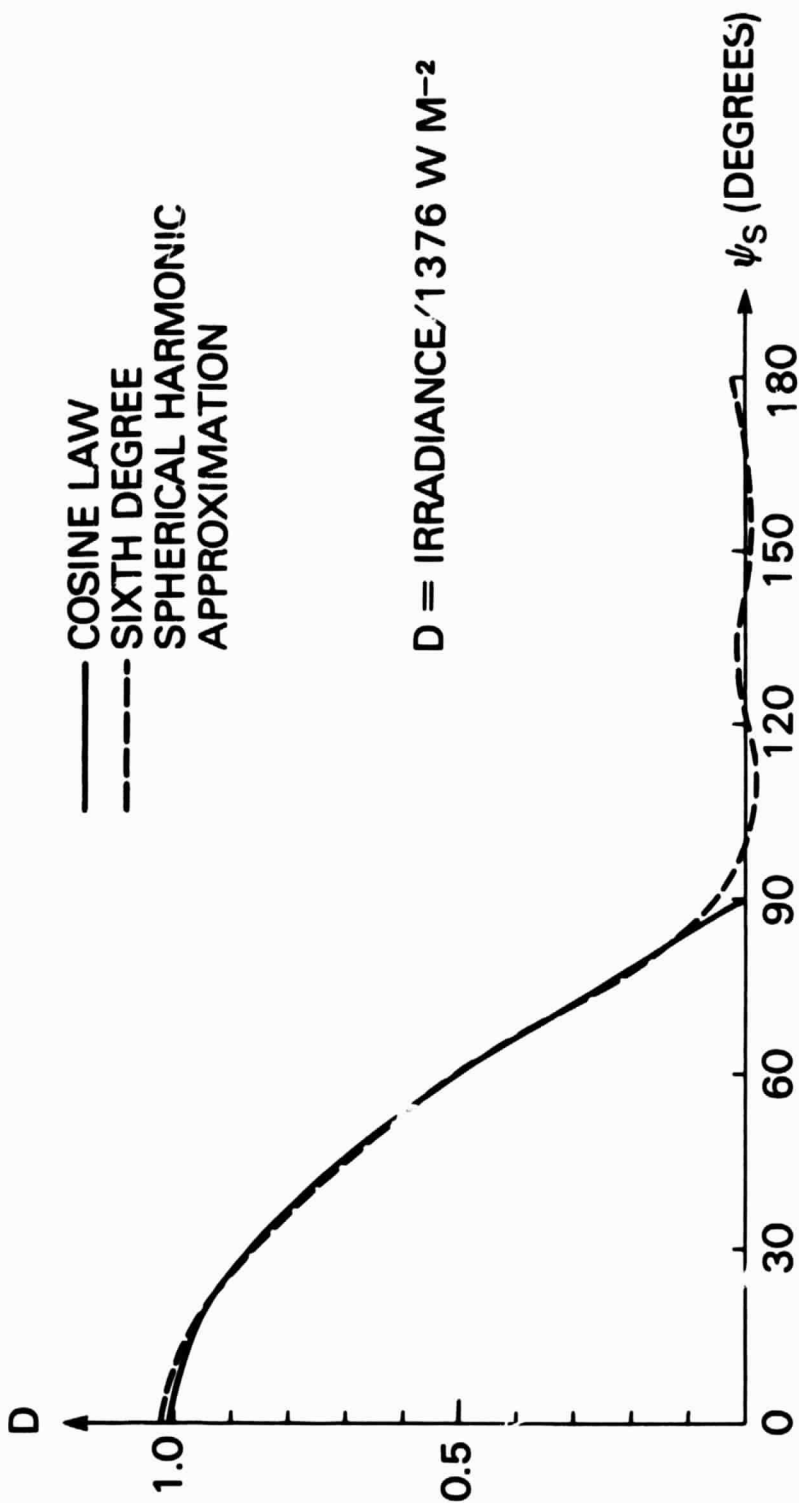
Figure 4. The function D (dashed line), for L summed between 0 and 6, and the exact function $\cos \psi_S$ (solid line), both plotted against ψ_S. D is basically the normalized solar irradiance.

Figure 5. The approximation for the function B (dashed line), for ℓ summed 0 and 6, and the exact function (solid line). Both are plotted against η. A circular orbit is assumed.

Figure 6. The coefficients $\overline{A}_{001}$ through $\overline{A}_{401}$ for each month. The error bars indicate one standard deviation. Arrows indicate error bars too big to fit on the graph. The larger errors are due to sparser data because of shadowing at either pole.

Figure 7. The time-averaged zonal albedo of Stephens et al. (1981) (solid line), and the time-averaged approximation used here (dashed line).

Figure 8. The radial acceleration R over one revolution for N = 0. The sun is on the equator and Lageos passes over the subpolar point.

Figure 9. The radial acceleration R over one revolution for N = 2. The sun is on the equator and Lagcos passes over the subpolar point.

Figure 10. The along-track acceleration S over one revolution for N = 0. The sun is on the equator and Lageos passes over the subpolar point.

Figure 11. The along-track acceleration S over one revolution for N = 2. The sun is on the equator and Lageos passes over the subpolar point.

Figure 12. The acceleration W (normal to the orbital plane) over one revolution for N = 2. the sun is on the equator and Lageos passes over the subpolar point.

Figure 13. The top graph shows the long-period changes in Lageos semimajor axis and eccentricity. The changes in a and e have virtually the same shape; hence only one graph is used for both. The bottom graph shows changes in inclination. Both graphs are for an earth with a uniform albedo (N = 0) and $\overline{A}_{001}$ = 0.3.

Figure 14. The long-period changes in the longitude of the Lageos node (top) and the argument of perigee (bottom) with time. The secular change in Ω is omitted. Both graphs are for N = 0, $\overline{A}_{001}$ = 0.3.

Figure 1. The Lageos satellite. Lageos is a completely passive satellite whose aluminum surface is studded with laser retroreflectors.

Figure 2. Positions of the sun, satellite, and surface element in the inertial coordinate system xyz. The coordinate system does not rotate around with the earth. The x-axis points to the vernal equinox and the z-axis lies along the rotation axis. Since the system is considered to be inertial, fictitious forces produced by the earth's motion around the sun are ignored.

Figure 3. The local frame $x_1 y_1 z_1$ of the surface element dS. The vector $\vec{r_1}$ and the circuit ABCD are discussed in Appendix 1; otherwise they are to be ignored.

NORMALIZED SOLAR IRRADIANCE

Figure 4. The function D (dashed line) for L summed between 0 and 6, and the exact function $\cos \psi_S$ (solid line), both plotted against ψ_S. D is basically the normalized solar irradiance.

FUNCTION B FOR LAGEOS

ACTUAL CURVE

SIXTH DEGREE
SPHERICAL HARMONIC
APPROXIMATION

$$B = \frac{\cos\eta - \rho}{[1 - 2\rho\cos\eta + \rho^2]^2}$$

η (DEGREES)

Figure 5. The approximation for the function B (dashed line), for ℓ summed between 0 and 6, and the exact function (solid line). Both are plotted against η. A circular orbit is assumed.

60

Figure 6. The coefficients $\bar{A}_{001}$ through $\bar{A}_{401}$ for each month. The error bars indicate one standard deviation. Arrows indicate error bars too big to fit on the graph. The larger errors are due to sparser data, because of shadowing at either pole.

Figure 7. The time-averaged zonal albedo of Stephens et al. (1981) (solid line), and the time-averaged approximation used here (dashed line).

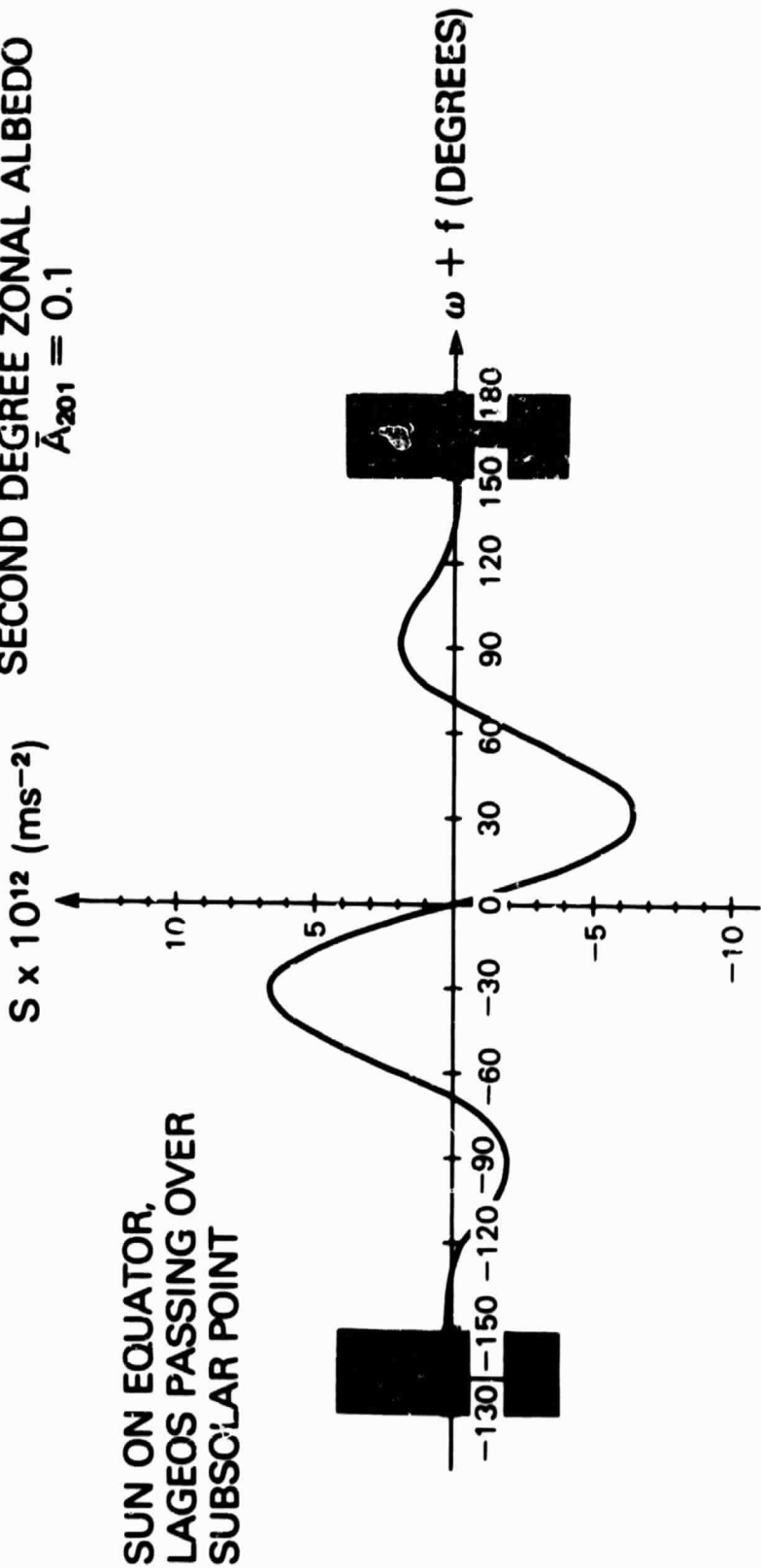Figure 8. The radial acceleation R over one revolution for N = 0. The sun is on the equator and Lageos passes over the subpolar point.

63

Figure 9. The radial acceleration R over one revolution for N = 2. The sun is on the equator and Lageos passes over the subpolar point.
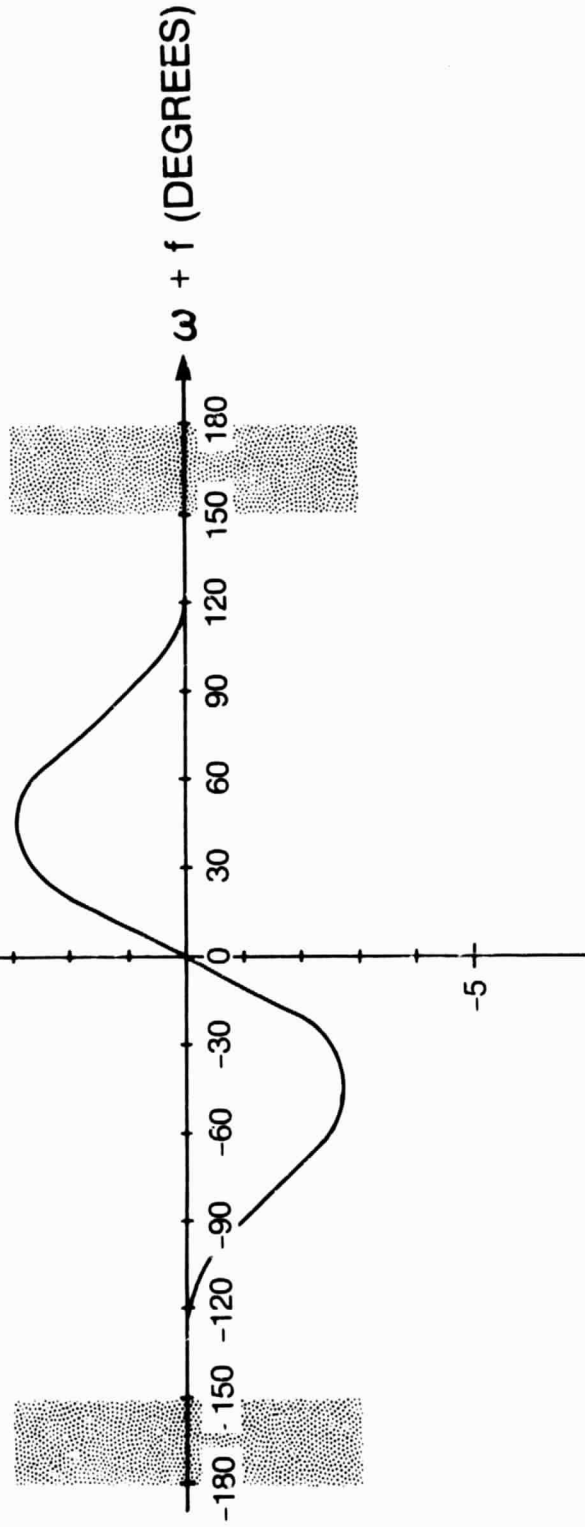
64

Figure 10. The along-track acceleration S over one revolution for N = 0. The sun is on the equator and Lageos passes over the subpolar point.

65

Figure 11. The along-track acceleration S over one revolution for N = 2. The sun is on the equator and Lageos passes over the subpolar point.

Figure 12. The acceleration W (normal to the orbital plane) over one revolution for N = 2. The sun is on the equator and Lageos passes over the subpolar point.

67

LAGEOS
CHANGES IN SEMIMAJOR AXIS,
ECCENTRICITY, AND INCLINATION
$\bar{A}_{001} = 0.3$

Figure 13. The top graph shows the long-period changes in the Lageos semimajor axis and eccentricity with time. The changes in a and e have virtually the same shape, hence only one graph is used for both. The bottom graph shows changes in inclination. Both graphs are for an earth with a uniform albedo (N = 0) and $\bar{A}_{001} = 0.3$.
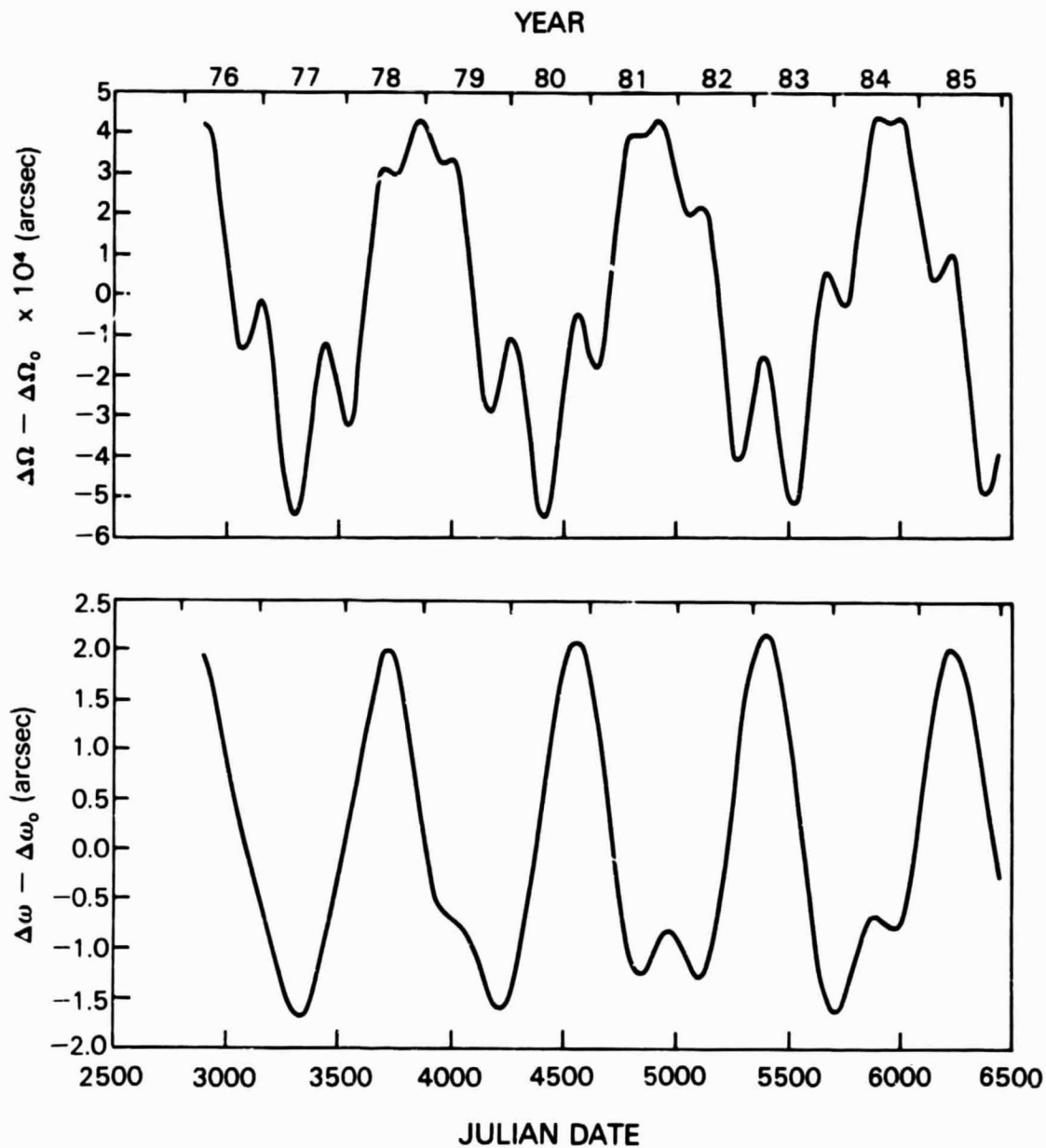
LAGEOS
CHANGES IN NODE (PERIODIC TERMS)
AND ARGUMENT OF PERIGEE
$\bar{A}_{001} = 0.3$

Figure 14. The long-period changes in the longitude of the Lageos node (to̶ nd the argument of perigee (bottom)
with time. The secular change in Ω is omitted. Both graphs are f   0, $\bar{A}_{001} = 0.3$.

1. Report No. TM 86210	2. Government Accession No.	3. Recipient's Catalog No.
4. Title and Subtitle Earth Albedo and the Orbit of Lageos		5. Report Date June 1985
		6. Performing Organization Code 621
7. Author(s) David Parry Rubincam and Nelson R. Weiss		8. Performing Organization Report No. 85B0381
9. Performing Organization Name and Address Geodynamics Branch, Code 621 Goddard Space Flight Center Greenbelt, MD 20771		10. Work Unit No.
		11. Contract or Grant No.
		13. Type of Report and Period Covered
12. Sponsoring Agency Name and Address NASA Goddard Space Flight Center Greenbelt, MD 20771		TM
		14. Sponsoring Agency Code

15. Supplementary Notes

Submitted to Celestial Mechanics

16. Abstract

The long-period perturbations in the orbit of the Lageos satellite due to the earth's albedo have been found using a new anlaytical formalism. The earth is assumed to be a sphere whose surface diffusely reflects sunlight according to Lambert's law. Specular reflection is not considered. The formalism is based on spherical harmonics; it produces equations which hold regardless of whether the terminator is seen by the satellite or not. Specializing to the case of a realistic zonal albedo shows that Lageos' orbital semimajor axis changes periodically by only a few millimeters and the eccentricity by one part in 10^5. The longitude of the node increases secularly by about 3×10^{-4} arc sec yr^{-1}. The effect considered here can explain neither the secular decay of 1.1 mm day^{-1} in the semimajor axis nor the observed along-track variations in acceleration of order 2×10^{-12} ms^{-2}.

17. Key Words (Selected by Author(s)) Albedo, Lambert's law, Lageos	18. Distribution Statement		
19. Security Classif. (of this report) Unclassified	20. Security Classif. (of this page) Unclassified	21. No. of Pages 70	22. Price*

*For sale by the National Technical Information Service, Springfield, Virginia 22161 GSFC 25-44 (10/77)